Qualitative Computing

Beyond and behind linear algebra

A summary of the activity of the Qualitative Computing group

2013 - 2014

Françoise Chatelin
Jean-Baptiste Latre
Monserrat Rincón-Camacho
Philippe Ricoux

CERFACS Project supported by the Direction Scientifique TOTAL

BEYOND AND BEHIND LINEAR ALGEBRA

A SUMMARY OF THE 2013-2014 ACTIVITY OF THE QUALITATIVE COMPUTING GROUP

CERFACS TECHNICAL REPORT TR/PA/14/80

FRANÇOISE CHATELIN [1,2], JEAN-BAPTISTE LATRE [1], M. MONSERRAT RINCON-CAMACHO [1], AND PHILIPPE RICOUX [3]

Abstract. Over the last century, linear algebra theory and matrix computations became irreplaceable, not only for high-tech industries, but also in every corner of our computerised society. Most of the time, any given problem (linear or not) is reduced to finding the solution of a linear system. Thus, the possibility of solving large linear systems in a reasonable amount of time using parallel algorithms has cast a shadow on any other kind of computing approach. However, physical problems are not linear in general: they often represent strongly coupled phenomena which inherently resist software parallelisation. Devising ways to overcome or circumvent computational difficulties has been the research core of the Qualitative Computing (QC) group at Cerfacs ever since it was established in 1987, [Chaitin-Chatelin and Frayssé, 1996, Chatelin, 2012a, Chatelin, 2012b, Chatelin, 2016]. In this summary we review some of the reasons why number tools other than matrices may be better fitted for extreme computing and how they offer a radically new perspective on the current field of linear algebra.

Keywords: multiplication, associative, commutative, ring, zerodivisor, idempotent, unipotent, nilpotent, triple nature of number plane, magnitude, elliptic, parabolic, hyperbolic, numbers, inherent parallelism, Cauchy-Riemann in $\mathbb{C}$ vs ${}^2\mathbb{R}$, spectral coupling in the bireal plane for symmetric matrices, hypercomplex, pluriduals, error-free derivation.

1. Multiplication and nonlinearity

The linear perception of the world governed by a one dimensional time is reflected by the preference of working with linear vector spaces where only scalar multiplication and vector addition $(+)$ are allowed. However multiplication $(\times)$ in a multidimensional algebra which yields nonlinearity is more fundamental than addition in Nature. The loss of information resulting from the mechanical use of linear causality may be one of the reasons behind the elusive physical phenomenon known as entropy in thermodynamics. Computation is mind's antidote to physical entropy [Chatelin, 2012b, Section 11.7.5].

By admitting multiplication into algebraic structures to create hypercomplex numbers [Cartan, 1908], new promising computation techniques appear. As early as 1870, Maxwell was well aware of the power of the noncommutative field of quaternions to express in a most elegant and shortest mathematical form the theory of electromagnetism. We recall that square matrices are just special cases of hypercomplex numbers. By harnessing the full power of matrix multiplication, the QR algorithm makes it possible to compute all roots at once of any polynomial of degree n, a feat not achieved by Newton's method which operates on *vectors*. The "miraculous"

(1) CERFACS, 42, avenue Gaspard Coriolis, 31057 Toulouse, France. (chatelin@cerfacs.fr, latre@cerfacs.fr, rincon@cerfacs.fr).

(2) CEREMATH, Université Toulouse 1 Capitole, 21, Allée de Brienne, 31000 Toulouse, France.

(3) TOTAL SA Direction Scientifique, 24, cours Michelet LA DEFENSE 10, 92069 Paris La Defense CEDEX, France. (philippe.ricoux@total.com).

QR algorithm is based on two key properties: (i) the stable Laplace *factorisation* $A = QR$, (ii) the *noncommutativity* of matrix $\times$, $A' = RQ = QAQ^T = Q'R'$, a process endlessly repeated.

The main creative jumps in the notion of $\times$ (hence of nonlinearity) that occurred historically over time are listed in Figure 1. It is worth noticing that concepts like 0 and the imaginary number i, $i^2 = -1$, so fruitful in modern applications, were a source of heated debate at the time they were introduced, [Chatelin, 2012b]. After 3 and a half millennia of slow evolution, one witnesses an *outburst* of new concepts during the 2^{nd} half of the 19^{th} century thanks to Hamilton and his quaternions $\mathbb{H}$, a noncommutative field in four dimensions and thanks to Graves and the octonions $\mathbb{G}$, a non associative (alternative) division algebra in 8D.

2000 B.C.	Sumer, implicit floating point notation; quadratic equations with positive discriminant
7^{th} to 12^{th} century	Brahmagupta to Bhaskara, 0 is a number
14^{th} C.	N. Oresme, $\frac{1}{0} = \infty$, $\zeta(1) = 1 + \frac{1}{2} + \ldots + \frac{1}{n} + \ldots = \infty$
16^{th} C.	Cardano, $i = \sqrt{-1}$, $x^2 + 1 = 0 \Rightarrow \mathbb{C} = \mathbb{R} \oplus i\mathbb{R}$
18^{th} C.	Euler, $e^{i\pi} + 1 = 0$, $\zeta(s)$ for $s > 1$, $\zeta(-2n) = 0$
1843	Hamilton, quaternions $\mathbb{H}$; Graves, octonions $\mathbb{G}$
1849	Cockle, $u = \sqrt{1}$, $u \neq \pm 1$, $\Rightarrow$ bireals ${}^2\mathbb{R} = \mathbb{R} \oplus u\mathbb{R}$
1873	Clifford, $n = \sqrt{0}$, $n \neq 0$, $\Rightarrow$ duals $\mathbb{D} = \mathbb{R} \oplus n\mathbb{R}$
1883	Weierstrass, zerodivisors
1891	Maxwell, electromagnetism in a nearly quaternion frame
1893	Scheffers, classical integral and differential calculus extends to arbitrary $\times \Leftrightarrow \times$ is associative and commutative
1903	Frobenius, hypercomplex numbers
1908	Cartan, encyclopedic review of algebras in arbitrary dimension
1912	Dickson, duplicating process
W.W.I.	
1927	Kasner, polygenic analysis
W.W.II.	
1960	Francis and Kublanovskaya, QR algorithm
1979	Lawson et al., Basic Linear Algebra Subprograms

FIGURE 1. Time line for $\times$

The complex numbers $\mathbb{C}$, the quaternions $\mathbb{H}$, the octonions $\mathbb{G}$, the bireals ${}^2\mathbb{R}$ [Cockle, 1848] and the duals $\mathbb{D}$ [Clifford, 1873] are some examples of the nonlinear algebras studied by the QC group in the past two years, see table on page 28. In this table, the hierarchical aspect of the algebras is highlighted together with their properties with respect to commutativity and associativity. Different physical applications have benefited from these variety of algebras thanks to their different characteristics [Latre, 2013]. For instance, the loss of commutativity in $\mathbb{H}$ reflects the non commutativity of a composition of 3D-rotations and the loss of associativity in $\mathbb{G}$ receives an interpretation in high energy physics [Baez, 2002]. Thus, with a broad spectrum of nonlinear algebras in mind, we aim to find a good match between the algebraic framework and the physical problem in accord with the mathematical qualities of the latter, instead of adapting the nonlinear physical problem to a linear algebra framework.

More of the work of QC (1987 to present) is presented at `http://hypnos.cerfacs.fr/videos/?video=MEDIA140522181700362`. In this summary, we focus on the recent research supported by the Direction Scientifique Total (2013-to present).

2. The hidden roots of a polynomial

The Fundamental Theorem of Algebra (FTA) states that over $\mathbb{C}$ a polynomial of degree n has n roots in $\mathbb{C}$, i.e. the field of complex numbers is algebraically closed. However over the bireal numbers ${}^2\mathbb{R}$ or over the dual numbers $\mathbb{D}$ (see Technical Annex A for their definition) which have a ring structure, the number of roots can be $> n$ if at least 2 distinct real roots exist. Then there exist "hidden" roots in rings which are not predicted by FTA. It may be computationally wiser not to ignore them.

As an example let us consider the quadratic polynomial with *real* coefficients

$$az^2 + bz + c = 0, \quad a, b, c \in \mathbb{R}, \tag{2.1}$$

with real discriminant $\Delta = b^2 - 4ac$, thus (2.1) has

- two complex conjugate roots $z_\pm = -\frac{b}{2a} \pm i\frac{\sqrt{|\Delta|}}{2a}$ if $\Delta < 0$ which are displayed in Figure 2 (a),
- two real roots $z_\pm = -\frac{b}{2a} \pm \frac{\sqrt{\Delta}}{2a}$ and two bireal rools $\hat{z}_\pm = -\frac{b}{2a} \pm u\frac{\sqrt{\Delta}}{2a}$ if $\Delta > 0$, Figure 2 (b),
- a double real root $z = -\frac{b}{2a}$ and an infinity of dual roots $\tilde{z} = -\frac{b}{2a} + ny$, $y \in \mathbb{R}$ if $\Delta = 0$, Figure 2 (c).

To verify that the "hidden roots" $\hat{z}_\pm \in {}^2\mathbb{R}$ and $\tilde{z} \in \mathbb{D}$ satisfy equation (2.1), one needs only to appley the multiplication rules given in A.1, with $\alpha = 1$, $\beta = 0$ for ${}^2\mathbb{R}$ and $\alpha = \beta = 0$ for $\mathbb{D}$.

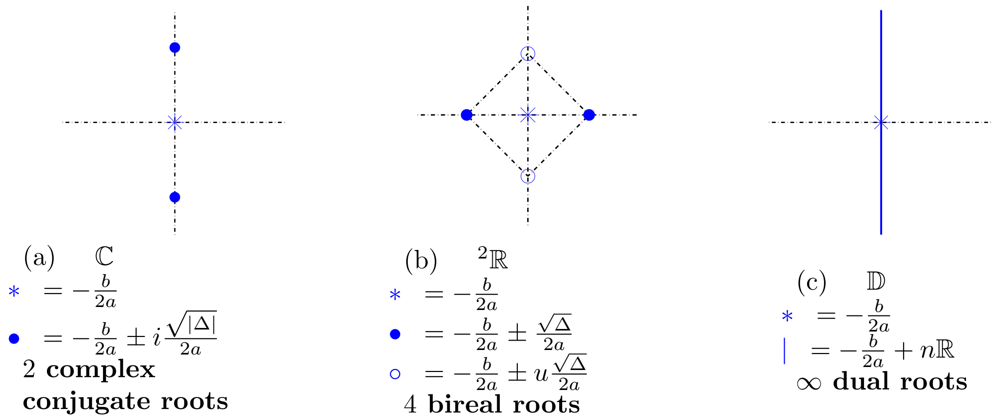

Figure 2. Polynomial roots in the numerical plane

Because so many significant engineering applications of complex numbers emerged over the last three centuries, the initial strong resistance to the idea that a square number could be negative vanished. In this spirit and to convince the skeptic reader, we present two compelling applications of the practical use of bireal and dual numbers for computation.

2.1. ${}^2\mathbb{R}$ **: Natural Parallelism.** A number $z = x + yu \in {}^2\mathbb{R}$, has the following idempotent representation

$$z = Xe_+ + Ye_-,$$

where $X = x + y$, $Y = x - y$ and $\{e_+, e_-\}$ (plotted in Figure 3) is an orthonormal basis given by

$$e_+ = \tfrac{1+u}{2}, \;\; e_- = \tfrac{1-u}{2}.$$

The elements in this basis are idempotent ($e_\pm^2 = e_\pm$) and zerodivisors ($e_+ \times e_- = 0$).

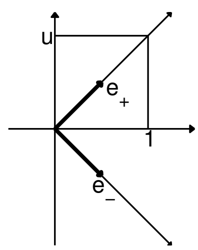

FIGURE 3. Idempotent basis

Under this idempotent representation, the multiplication is done *componentwise*

$$\begin{aligned} zz' &= (x + yu)(x' + y'u) \\ &= (Xe_+ + Ye_-)(X'e_+ + Y'e_-) \\ &= XX'e_+ + YY'e_-, \end{aligned}$$

and consequently

$$\begin{aligned} z^k &= (x + yu)^k \\ &= (Xe_+ + Ye_-)^k \\ &= X^k e_+ + Y^k e_- \end{aligned}$$

where $k \in \mathbb{N}^*$. Likewise, the idempotent representation of a bireal polynomial P is

$$P(z) = P_+(X)e_+ + P_-(Y)e_-, \;\; X = x + y, \;\; Y = x - y$$

where the roots of P are completely determined by the real roots of the polynomials with real coefficients P_+ and P_- which are independent from each other.

Furthermore, an iterative construction allows us to extend this idempotent representation into higher dimensions 2^k, $k \geq 2$ and we obtain the *multiplanar numbers* [Chatelin, 2016] (B.3 last three columns, in table page 28): Let $R_1 \in \{\mathbb{C}, {}^2\mathbb{R}, \mathbb{D}\}$ be a planar ring of dimension $n = 2$. Given R_{k-1} and an unipotent $\mathbf{u}_k \notin R_{k-1}$, $\mathbf{u}_k^2 = 1$ of dimension 2^k, then

$$R_k = R_{k-1}[\mathbf{u}_k] = R_{k-1} \oplus R_{k-1}\mathbf{u}_k$$

is a commutative ring where $\mathbf{u}_k$ is the k^{th} generator. For a unipotent generator $\mathbf{u}_j$, $2 \le j \le k$, the corresponding idempotent vectors are $\mathbf{e}_j^{\pm} = \frac{1}{2}(1 \pm \mathbf{u}_j)$ and we define the sets:

$$\begin{aligned} E_1 &= \{\mathbf{e}_k^{\pm}\} \\ E_2 &= \mathbf{e}_{k-1}^{+} E_1 \cup \mathbf{e}_{k-1}^{-} E_1 = \{\mathbf{e}_{k-1}^{+}\mathbf{e}_k^{\pm}, \mathbf{e}_{k-1}^{-}\mathbf{e}_k^{\pm}\} \\ &\vdots \\ E_l &= \mathbf{e}_{k-(l-1)}^{+} E_{l-1} \cup \mathbf{e}_{k-(l-1)}^{-} E_{l-1} \\ &\vdots \\ E_{k-1} &= \mathbf{e}_2^{+} E_{k-2} \cup \mathbf{e}_2^{-} E_{k-2} \end{aligned}$$

thus, an element $x \in R_k$, $k \ge 2$ has $k-1$ idempotent representations of the 2^l idempotents $\{\mathbf{e}_j^{(l)}\}$ in E_l, $1 \le l \le k-1$

$$x = \sum_{j=1}^{2^l} x_j^{(l)} e_j^{(l)}, \quad x_j^{(l)} \in R_{k-1}, \quad e_j^{(l)} \in E_l.$$

Hence, this representation shows a natural parallelism where the multiplication of two elements of dimension 2^k, $x, y \in R_k$, $x = \sum_{j=1}^{2^l} x_j^{(l)} e_j^{(l)}$ and $y = \sum_{j=1}^{2^l} y_j^{(l)} e_j^{(l)}$ is done componentwise:

$$xy = \sum_{j=1}^{2^l} x_j^{(l)} y_j^{(l)} e_j^{(l)}.$$

2.2. $\mathbb{D}$ **: Error free derivatives.** The use of complex numbers for the derivative computation has been already studied in [Martins et al., 2003, Lantoine et al., 2012]. In order to compute the derivative of a function $f : \mathbb{R} \to \mathbb{R}$ at a point x, this function is extended over the complex numbers. Numerically this is done by overloading operators and functions in a given programming language. The Taylor expansion around x is as follows for $h \in \mathbb{R}$

$$f(x+hi) = f(x) + f'(x)hi - \tfrac{f''(x)}{2!}h^2 - \tfrac{f'''(x)}{3!}h^3 i + \ldots + \tfrac{f^{(k)}(x)}{k!}h^k i^k + \ldots$$

with imaginary part

$$\mathrm{Im}[f(x+hi)] = f'(x)h - \tfrac{f'''(x)}{3!}h^3 + \tfrac{f(5)(x)}{5!}h^5 + \ldots, \quad \mathrm{Im} = \text{imaginary part}$$

Then, the derivative of f at x is:

$$f'(x) = \tfrac{\mathrm{Im}[f(x+hi)]}{h} + \mathcal{O}(h^2), \tag{2.2}$$

This process can be generalised for higher order derivatives by means of Multicomplex numbers ($C_k = {}^{2^{k-1}}\mathbb{C}$, $C_1 = \mathbb{C}$ in table page 28), see [Lantoine et al., 2012].

Analogously one may extend the function f over the bireal numbers to obtain

$$f(x+hu) = f(x) + f'(x)hu + \tfrac{f''(x)}{2!}h^2 + \tfrac{f'''(x)}{3!}h^3 u + \ldots + \tfrac{f^{(k)}(x)}{k!}h^k u^k + \ldots,$$

from where the unreal part is

$$\mathrm{Un}[f(x+hu)] = f'(x)h + \tfrac{f'''(x)}{3!}h^3 + \tfrac{f'''(x)}{5!}h^5 + \ldots, \quad \mathrm{Un} = \text{unreal part}$$

and the first derivative

$$f'(x) = \tfrac{\mathrm{Un}[f(x+hu)]}{h} + \mathcal{O}(h^2). \tag{2.3}$$

If the dual numbers are used as proposed in [Dimentberg, 1965, Dimentberg, 1968, Fike, 2013], the Taylor expansion around x is simply

$$f(x) = f(x) + f'(x)hn,$$

from where

$$\mathrm{Un}[f(x+hn)] = f'(x)h$$

and

$$f'(x) = \tfrac{\mathrm{Un}[f(x+hn)]}{h}. \tag{2.4}$$

Therefore, there are no truncation error and no subtractive cancellation error.

In order to test these results, we consider the function

$$f(x) = \frac{e^x}{\sqrt{\sin^3 x + \cos^3 x}}, \quad f'(x) = \frac{e^x(3\cos x + 5\cos 3x + 9\sin x + \sin 3x)}{8(\sin^3 x + \cos^3 x)^{\frac{3}{2}}}$$

which is extended to $\mathbb{C}$, ${}^2\mathbb{R}$ and $\mathbb{D}$

$$f(z) = v(x,y) + w(x,y)g, \quad g \in \{i,u,n\}.$$

According to (2.2), (2.3) and (2.4), the approximative derivative is given by $\frac{w(x,y)}{y}$ and the approximation error is

$$E(x,y) = \|f'(x) - \tfrac{w(x,y)}{y}\|.$$

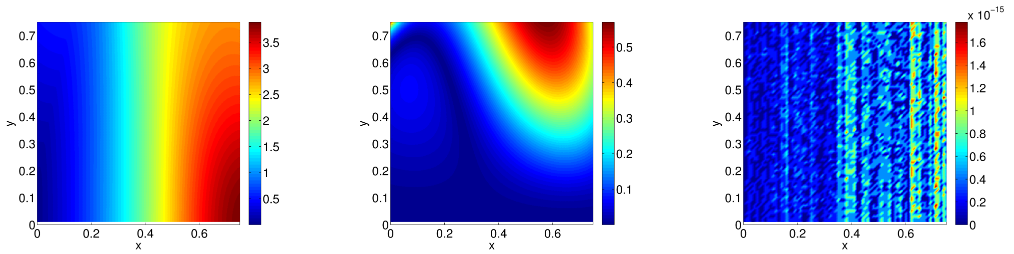

(a) $z \in \mathbb{C}$, $E(x,y) \leq 4$ (b) $z \in\ {}^2\mathbb{R}$, $E(x,y) \leq 0.6$ (c) $z \in \mathbb{D}$, , $E(x,y) \leq 10^{-15}$

FIGURE 4. Derivative approximation error

In Figure 4, the approximation error is displayed for $(x,y) \in [0, 0.75]^2$. Readily we see that the best option is when the function f is extended to the dual numbers, where the error $E(x,y)$ is of the order of machine epsilon 10^{-15}, Figure 4 (c). The reason of this surprising results is due to the Cauchy Riemann (CR) conditions in $\mathbb{D}$ described in A.2. Let $z = x + yn \in \mathbb{D}$ be in a domain $U \subset \mathbb{R}^2$ and suppose $f(z) = v(x,y) + w(x,y)n$ to be C^1, i.e. $v, w \in C^1(U)$, thus the (CR) conditions are $v_x = w_y$, $v_y = 0$ and f is of the form

$$f(x + y\,n) = f(x) + f'(x)y\,n,$$

for any $y \in \mathbb{R}$, not only small as it is usually supposed in the derivative approximation by Taylor series. For example, the real functions $\exp(x)$, $\sin(x)$, x^k extended over $\mathbb{D}$ are as follows:

$$\begin{aligned}
\exp(x+yn) &= \exp(x) + \exp(x)yn,\\
\sin(x+yn) &= \sin(x) + \cos(x)yn,\\
(x+yn)^k &= x^k + kx^{k-1}yn.
\end{aligned}$$

Moreover, it is possible to recursively compute higher order derivatives by means of the *pluridual* numbers $\mathbb{D}^{(k)} = \mathbb{D}^{(k-1)}(\mathbb{D})$ (first column in table page 28), already exploited in the movie industry, [Piponi, 2004]. If $k = 2$, $z \in \mathbb{D}^{(2)} = \mathbb{D}(\mathbb{D})$, then, if we introduce *two* orthogonal nilpotent units n_1 and n_2, we get

$$z = y_0 + n_2 y_1, \quad y_0, y_1, \in \mathbb{D} \text{ defined by } n_1$$
$$z = (x_0 + x_1 n_1) + n_2(x_2 + x_3 n_1), \quad n_1^2 = 0, \;\; n_2^2 = 0, \;\; (n_1 n_2)^2 = 0$$

and a function $f : \mathbb{D}^{(2)} \mapsto \mathbb{D}^{(2)}$ is given by

$$\begin{aligned} f(z) &= f(y_0 + n_2 y_1) \\ &= f(y_0) + n_2 f'(y_0) y_1 \end{aligned}$$

where

$$f(y_0) = f(x_0 + x_1 n_1) = f(x_0) + n_1 f'(x_0) x_1, \qquad f'(y_0) = f'(x_0 + x_1 n_1) = f'(x_0) + n_1 f''(x_0) x_1.$$

Thus, for $z = x_0 + h_1 n_1 + h_2 n_2 \in \mathbb{D}^{(2)}$ it can be proved that:

$$f(x_0 + h_1 n_1 + h_2 n_2) = f(x_0) + h_1 f'(x_0) n_1 + h_2 f'(x_0) n_2 + h_1 h_2 f''(x_0) n_1 n_2.$$

from where we obtain the second order derivative:

$$f''(x_0) = \frac{\mathrm{Un}_{n_1 n_2} f(x_0 + h_1 n_1 + h_2 n_2)}{h_1 h_2}$$

and in general:

$$f^{(k)}(x_0) = \frac{\mathrm{Un}_{n_1 n_2 \cdots n_k} f(x_0 + h_1 n_1 + \ldots + h_k n_k)}{h_1 h_2 \cdots h_k}$$

for $x_0 + h_1 n_1 + \ldots + h_k n_k \in \mathbb{D}^{(k)}$.

3. Field vs. ring structures

The numerical plane enjoys *three* kinds of algebraic structures (Annex A.1), exemplified by the field $\mathbb{C}$ and the rings ${}^2\mathbb{R}$ or $\mathbb{D}$. Why is it that FTA addresses only the case of a *field*, be it $\mathbb{R}$ or $\mathbb{C}$?

The main difference between a field and a ring is that, in the latter structure, some nonzero elements have *no* inverse. We recall that an invertible x is such that $x \times x^{-1}_{\text{right}} = 1 = x^{-1}_{\text{left}} \times x$, with $x^{-1} = x^{-1}_{\text{left}} = x^{-1}_{\text{right}}$ when $\times$ is commutative. Does the lack of general invertibility create a serious computational difficulty?

Not really when the only non invertible elements are zerodivisors. Any $x \neq 0$ such that there exists $y \neq 0$ satisfying $x \times y = 0$ or $y \times x = 0 \neq 1$ is a nonzero zerodivisor. Such rings are called *classical* [Lam, 1999] in abstract algebra. All commutative rings of multiplanar numbers are classical, as well as the noncommutative ring of the square matrices of order n, $n \geq 2$. In the latter case, the set of zerodivisors consists of all non invertible matrices A with rank r, $1 \leq r < n$: $AB = 0$ for any $B \neq 0$ such that its range $\mathrm{Im}\, B \subseteq \mathrm{Ker}\, A$ of dimension $n - r > 0$. This set contains nilpotent matrices $N \neq 0$, $N^k = 0$ for some $k > 1$ and idempotent or projection matrices P, such that $P^2 = P$. These two notions, ubiquitous in linear algebra, originate clearly in the two *unreal* units u ($u^2 = 1$, $u \neq \pm 1$) and n ($n^2 = 0, n \neq 0$) invented with very little success by Cockle in 1848 and by Clifford in 1873 respectively. We recall that $e_\pm = \frac{1 \pm u}{2}$ are idempotent ($e_\pm^2 = e_\pm$) and zerodivisors ($e_+ e_- = 0$).

In retrospect, it seems surprising that the *implicit* preference of the 19^{th} century mathematical community for the field $\mathbb{C}$ rather than the rings ${}^2\mathbb{R}$ or $\mathbb{D}$ has survived until this day, despite the revolution of abstract algebra in the 20^{th} century...

4. Coupling

The term coupling indicates an interaction of two (or more) processes: physical phenomena (vibratory movements, light, sound or electricity), chemical reactions or mechanical systems among others. More generally, coupling designates how 2 or more items become entangled and how a new entity may emerge. In [Chaitin-Chatelin and Frayssé, 1996] the coupling of exact numerical methods with finite precision computations is studied in the neighbourhood of algebraic singularities, see Section 4.1 below. However coupling reflects the diversity of life itself which ultimately breaks any conceptual box that was conceived to frame, hence "explain" it. We content ourselves to refer the reader to Section B of the Technical Annex where several algebraic duplicating processes are presented. In the next three Sections 4.1 to 4.3 we present three very different applications of the idea of coupling to square matrices.

4.1. **High nonnormality against natural parallelism.** A matrix resulting from the discretisation of a partial differential operator, can inherit its nonnormality from a strong coupling between two physical phenomena which produces physical instabilities. Three classical examples of this situation are: one-dimensional convection-diffusion [Reddy and Trefethen, 1994], controlled fusion of plasma [Kerner, 1986, Kerner, 1989] and flutter [Braconnier et al., 1995]. In these cases, the spectrum of a family of operators depends on a parameter related to the coupling process and it exhibits a discontinuity as the parameter tends to a critical limit (often 0 or ∞).

A numerical example of the consequence of nonnormality the computed spectrum of a family of matrices is described in [Chatelin, 2012a, chapter 4]. The parameter $\nu > 0$ quantifies the amount of nonnormality of S_ν, the real Schur form of order $n = 2p$ defined by

$$S_\nu = \begin{pmatrix} x_1 & y_1 & & & & & & \mathbf{0} \\ -y_1 & x_1 & \nu & & & & & \\ & & x_2 & y_2 & & & & \\ & & -y_2 & x_2 & \nu & & & \\ & & & & \ddots & \ddots & & \\ & & & & \ddots & \ddots & \nu & \\ & & & & & & x_p & y_p \\ \mathbf{0} & & & & & & -y_p & x_p \end{pmatrix},$$

where $x_k = -\frac{(2k-1)^2}{1000}$, $y_k = \frac{2k-1}{100}$, $k = 1, \ldots, p$. The peculiarity of this matrix is that two consecutive blocks $\begin{bmatrix} x_k & y_k \\ -y_k & x_k \end{bmatrix}$ and $\begin{bmatrix} x_{k+1} & y_{k+1} \\ -y_{k+1} & x_{k+1} \end{bmatrix}$ are coupled by the parameter ν, the larger the value of ν, the stronger the coupling between blocks. Let us consider $A_\nu = QS_\nu Q^T$, where Q is the symmetric orthonormal matrix consisting of the eigenvectors of the second-order difference matrix

$$q_{ij} = \sqrt{\tfrac{2}{n+1}} \sin\left(\tfrac{ij\pi}{n+1}\right), \quad i, j = 1, \ldots, n.$$

A_ν and S_ν have the same spectrum, their exact eigenvalues are $x_k \pm iy_k$, independent of ν, plotted in red in Figure 5 for $n = 20$. The eigenvalues for $\nu = 1$, 10, 10^2 and 10^3 are computed by the backward stable algorithm QR; they are plotted in blue in Figure 5 (a), (b), (c), and (d) respectively. We obtain a clear example of an unstable spectrum due to the coupling parameter ν: the exact spectrum (in red) lying on a parabola is *computed* as lying on a circle (in blue) as ν increases enough ($\nu \geq 10^3$). Finite precision is *not* the cause of the discrepancy between the parabola and the circle. It only serves to reveal the inherent instability of the exact spectrum due to high nonnormality.

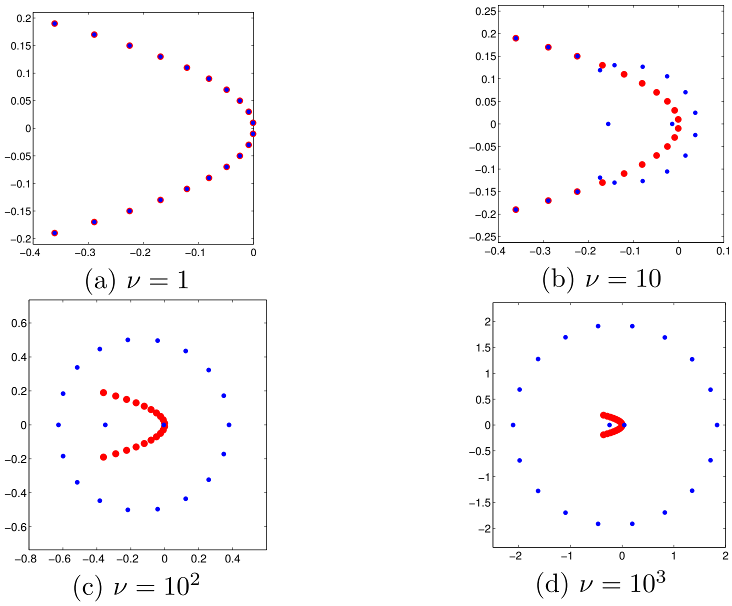

(a) $\nu = 1$ (b) $\nu = 10$

(c) $\nu = 10^2$ (d) $\nu = 10^3$

FIGURE 5. Exact (red) and computed (blue) eigenvalues of A_ν, $n = 20$

Therefore, any strong coupling which yields, under discretisation, a highly nonnormal matrix, cannot be safely cut into independent pieces: it resists natural parallelisability, [Chaitin-Chatelin and Frayssé, 1996, Chatelin, 2012a]. To overcome this limitation of matrices in linear algebra, the QC group explores the potential of multiplanar numbers, (Section 2.1), since they enable the user to process information in a hierarchical and naturally parallel fashion.

4.2. **Homotopic Deviation.** Another example of coupling is given by the family $A(t) = A + tE$ where a matrix $A \in \mathbb{C}^{n\times n}$ is coupled with a deviation matrix $E \in \mathbb{C}^{n\times n}$ of rank r, $1 \le r \le n$ by means of a parameter $t \in \hat{\mathbb{C}} = \mathbb{C} \cup \{\infty\}$, which expresses the intensity of the coupling. In [Chatelin, 2012b, chapter 7], it is shown that, when $1 \le r < n$, at most $g = n - r$ eigenvalues of $A + tE$ do not escape to infinity when $|t| \to \infty$; g is the geometric multiplicity of 0 as an eigenvalue of E, $1 \le g \le n-1$. This novel theory is more general than the classical perturbation theory where $|t| \in [0,1]$ and $\|E\|$ is small. It shows that when E is *singular* and $\lambda(t) \not\to \infty$, any limit point $\lambda(\infty) \in \mathbb{C}$ gives spectral information at finite distance about the synthesis $\lim_{t\to\infty} A + tE$ which cannot receive any mathematical meaning. For an application of this Homotopic Deviation theory in acoustics, see [Chaitin-Chatelin and Van Gijzen, 2006].

The complex evolution of $t = \rho e^{i\theta}$ yields the spectral field $t \in \hat{\mathbb{C}} \mapsto \lambda(t) = \lambda(\rho, \theta) \in \hat{\mathbb{C}}$. To ease the 2D-representation of the field we consider two families of planar curves: (i) spectral *rays* for θ fixed and $0 < \rho \le \infty$ and (ii) spectral *orbits* for $\rho > 0$ fixed and $0 \le \theta < 2\pi$. Their behaviours are illustrated in Figures 6 [Chatelin, 2012b, Example 7.12.1 and 7.5.5]. A of order 11 is the companion matrix of the polynomial $\pi(z) = z^{11} + 1$ and $V = [e_{11}, e_3]$, $U = [e, e_2]$, where e_i is the i^{th} canonical vector and $e = (1, \ldots, 1)^T$, $E = UV^T = [0, 0, e_2, 0, \ldots, 0, e]$ with rank $r = 2$, $g = 11 - 2 = 9$.

In Figure 6, the eigenvalues of A, (i.e. 11 roots of $\pi(z)$) are plotted in black, the four rays for $\theta = \frac{\pi}{3}, \frac{\pi}{5}, \frac{\pi}{8}, \frac{6\pi}{7}$ are plotted in (a) and the four orbits for $\rho = 1, 2, 4, 8$ in (b). Figure 6 illustrates that the real eigenvalue -1 is invariant under tE: $\lambda(t) = -1$ for all $t \in \mathbb{C}$. It displays the 7 limit points which are 0 and 6 points on the unit circle, near some of the original eigenvalues of $A(0) = A$. Four eigenvalues escape to ∞.

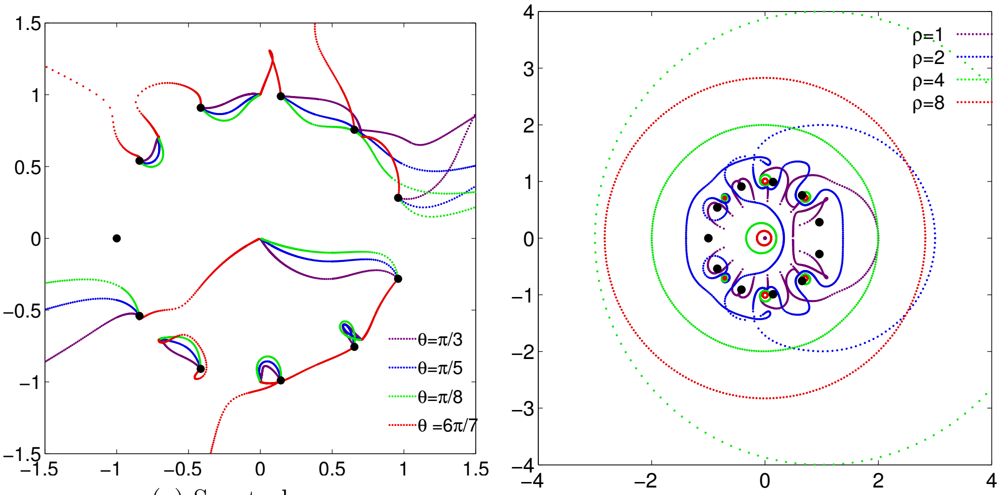

(a) Spectral rays (b) Spectral orbits

FIGURE 6. Eigenvalues of $A + tE$, $\rho e^{i\theta} = t \in \hat{\mathbb{C}}$

4.3. **Spectral coupling for a symmetric matrix.** Section 4.2 has treated the influence on the spectrum of the coupling between *two* matrices A and E. We now turn to the internal coupling of *two* eigenvalues for one symmetric matrix $A = A^T$ of order $n \geq 2$.

4.3.1. *Coupling two real eigenvalues.* According to Section 2, the quadratic polynomial with real coefficients

$$P(z) = z^2 - 2az + g^2, \tag{4.1}$$

has two complex conjugate roots when $\Delta = a^2 - g^2 < 0$ in conformity with FTA's prediction. However when $\Delta = 0$, it has a double root and an infinity of dual roots and when $\Delta = a^2 - g^2 > 0$, it has two real roots λ and λ' which can be *coupled* to form two bireal roots $\sigma_\pm = \frac{\lambda+\lambda'}{2} \pm \frac{\lambda'-\lambda}{2}u$ with magnitude $\mu(\sigma_\pm) = \sigma_+\sigma_- = g^2$ ($\sigma_+^* = \sigma_-$) when $\lambda \neq \lambda'$. Since $a = \frac{\lambda+\lambda'}{2}$ and $g^2 = \lambda\lambda'$, thus for $\Delta > 0$

$$P(z) = z^2 - 2az + g^2 = (z - \lambda)(z - \lambda') = (z - \sigma_+)(z - \sigma_-).$$

Here we illustrate on a symmetric matrix A how the existence of hidden eigenvalues $\sigma_\pm$ in ${}^2\mathbb{R}$ resulting from coupling the existing real ones $\lambda \neq \lambda'$ increases the amount of spectral information.

4.3.2. *Elementary geometry.* We summarise the results obtained from elementary geometry in the bireal plane [Chatelin, 2012a, chapter 8]; they are separated into two cases $\lambda\lambda' > 0$ and $\lambda\lambda' < 0$ and $|\lambda| \neq |\lambda'|$. A complete description, for double real roots and a null root are found in [Chatelin, 2016]. As before $a = \frac{\lambda+\lambda'}{2}$ is the arithmetic mean, $g^2 = \lambda\lambda'$ (g is the geometric mean when $\lambda\lambda' > 0$) and $e = \frac{\lambda'-\lambda}{2}$ is the distance of the couple $\{\lambda, \lambda'\}$ to the mean a.

(i) Case $g^2 = \lambda\lambda' > 0$, $0 \notin [\lambda, \lambda']$: The four roots λ, λ', $\sigma = \sigma_+$ and $\sigma^* = \sigma_-$ are plotted in the *bireal spectral plane* as shown in Figure 7 (a). The angle $\phi = \measuredangle(OC, OM)$, $0 < \phi < \frac{\pi}{2}$ is the angular information from O and $\cos\phi = \frac{g}{|a|}$. A complementary information is given by the angle $\psi = \measuredangle(MC, MO)$ which in this case is equal to $\frac{\pi}{2}$ and $\cos\psi = 0$.

(ii) Case $g^2 = \lambda\lambda' < 0$, $0 \in [\lambda, \lambda']$: When coupling two eigenvalues with opposite signs, the angle $\phi = \measuredangle(OC, OM)$ is equal to $\frac{\pi}{2}$ as plotted in Figure 7 (b). In this case the angle $\psi = \measuredangle(MO, MC)$ is such that $0 < \psi < \frac{\pi}{2}$ and $\cos\psi = \frac{|g|}{e}$.

A geometric interpretation is given below. A comparison between Fig. 7 (a) and 7 (b) shows that the roles of $|a|$ and e are exchanged in relation with the angles ψ and ϕ. Moreover, $g^2 = \mu(\sigma_\pm)$ is the power of O relative to the circle Γ passing through the 4 eigenvalues $\{\lambda, \lambda', \sigma_\pm\}$.

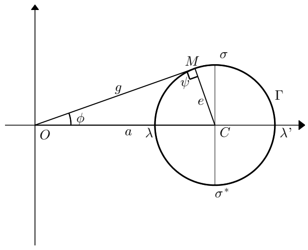

(a) $\phi = \measuredangle(OC, OM)$,
$\cos\phi = \frac{\langle v, Av\rangle}{\|v\|\|Av\|} = \frac{g}{|a|}$, $\cos\psi = 0$

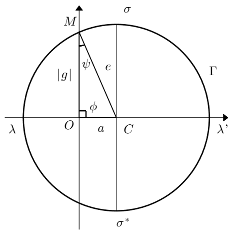

(b) $\psi = \measuredangle(MO, MC)$,
$\cos\psi = \frac{|g|}{e}$, $\cos\phi = 0$

FIGURE 7. Bireal spectral plane

4.3.3. *Spectral evolution in the invariant plane.* Now let us consider two orthogonal and normalised eigenvectors x and x' associated with $\lambda < \lambda'$ respectively. Thus, $\{x\}$ and $\{x'\}$ are invariant directions under A which span the invariant *plane* $\mathbf{M}$. The angular information of ϕ and ψ coming from coupling λ and λ' in the bireal spectral plane described in the previous section, is transferred to $\mathbf{M}$ in the following way.

Let us consider the unit circle $(C) = \{y = wx + w'x', \;\; w^2 + w'^2 = 1\}$ in $\mathbf{M}$ and the matrix $B = A - aI$. It can be shown that $\forall y \in (C)$: $\|By\| = e$. In Figure 8 in the plane $\mathbf{M}$, the vector ay is plotted in black for $y \in (C)$, its image Ay is plotted as a dotted black line and the vector By is displayed in red. A natural question is: when does the direction of y differ the most from the direction of Ay? To answer this question, let us consider the angles between the directions of the vectors y, Ay and By: $\alpha = \measuredangle(y, Ay)$, $\beta = \measuredangle(By, Ay)$ and $\gamma = \measuredangle(y, By)$ as displayed in Figure 8 (a). Thus, the direction of y differs the most from the direction of Ay when the angle α is the closest to $\frac{\pi}{2}$.

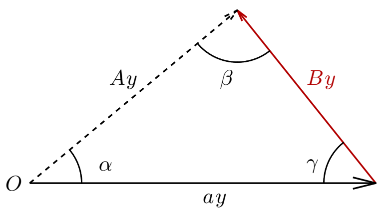

(a) $\alpha, \beta, \gamma \neq \frac{\pi}{2}$

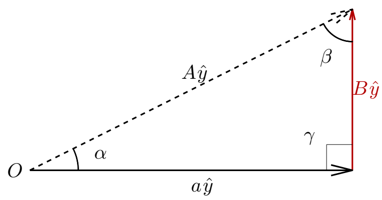

(b) $\gamma = \frac{\pi}{2}$, $\hat{y} \in E$

FIGURE 8. $y \in (C)$, $\|y\| = 1$, $\|By\| = e$

In the circle (C), there are 3 subset of 4 points to be distinguished:

$$\begin{array}{rcl} D_+ & = & \{v = \varepsilon w_+ x + \varepsilon' w'_+ x', \;\; \varepsilon \text{ and } \varepsilon' = \pm 1\}, \\ D_- & = & \{v = \varepsilon w_- x + \varepsilon' w'_- x', \;\; \varepsilon \text{ and } \varepsilon' = \pm 1\}, \\ E & = & \{y = \frac{1}{\sqrt{2}}(\varepsilon x + \varepsilon' x'), \;\; \varepsilon \text{ and } \varepsilon' = \pm 1\}, \end{array}$$

displayed in Figure 9 over the invariant plane $\mathbf{M}$, where:

i. $w_+^2 = \frac{\lambda'}{2a}$ and $w_+'^2 = \frac{\lambda}{2a}$ if $g^2 > 0$,
ii. $w_-^2 = \frac{\lambda'}{2e}$ and $w_-'^2 = -\frac{\lambda}{2e}$ if $g^2 < 0$.

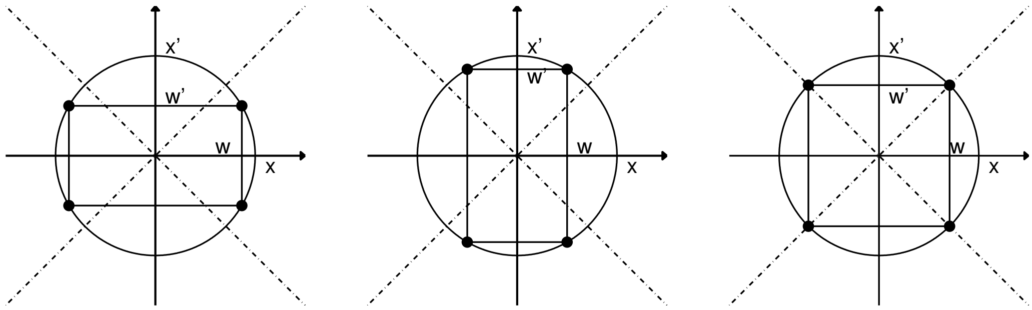

(a) $D_+ \subset (C)$, $g^2 > 0$, $a > 0$ (b) $D_- \subset (C)$, $g^2 < 0$, $-\lambda > \lambda'$ (c) $E \subset (C)$, $w = w'$

FIGURE 9. In the invariant plane $\mathbf{M} = \{x, x'\}$

An element $v \in D_+$ (case $g^2 > 0$) has the following properties: $\|Av\| = |g|$, $\langle v, Av\rangle = \frac{g^2}{a}$, $\langle Bv, Av\rangle = 0$, $\cos\phi = \frac{v, Av}{\|v\|\|Av\|} = \frac{g}{a}$ and $\cos\psi = 0$ ($\psi = \frac{\pi}{2}$), see Figure 7 (a) and Figures 10 (c) and 11 (c) for examples. Moreover any v in D_+ minimises $|\cos\alpha|$ over $\mathbf{M}$ where $\cos\alpha$ is the functional

$$0 \neq y \in \mathbb{R}^n \setminus \text{Ker } A \mapsto \cos\alpha(A, y) = \frac{y^T Ay}{\|y\|\|Ay\|} \tag{4.2}$$

whose Euler's equation is

$$\frac{A^2 y}{\|Ay\|^2} - 2\frac{Ay}{\langle y, Ay\rangle} + \frac{y}{\|y\|^2} = 0, \quad 0 \neq y \in \mathbb{R}^n \setminus \text{Ker } A. \tag{4.3}$$

The angle ϕ is called the *outer turning* angle because it corresponds to the maximum angle between v and its image Av for $v \in D_+$ and $0 \notin [\lambda, \lambda']$: v is called a *catchvector*. This angular information ϕ is an outer measure of the *elasticity* of A. Moreover since $\psi = \frac{\pi}{2}$, ϕ and ψ are extremal values for α and β. The four catchvectors in D_+ are illustrated in Figures 10 (d) and 11 (d) together with their image Av in a dotted line and the vector Bv, the four triplets (av, Av, Bv) are displayed in four different colours, blue, green, yellow and magenta. A comparison with Figure 10 (a), clearly see that the angles $\alpha = \phi = \measuredangle(v, Av)$ and $\beta = \psi = \measuredangle(Bv, Av)$ are extremal for v in D_+. In Figures 10 and 11, the right triangle OMC in (c) is equal to the right triangle formed by av, Bv and Av in (d).

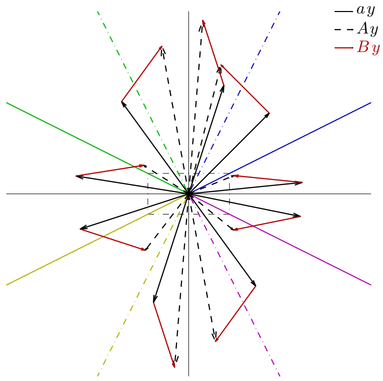

(a) $y \in (C)$, ay, Ay and By in $\mathbf{M}$

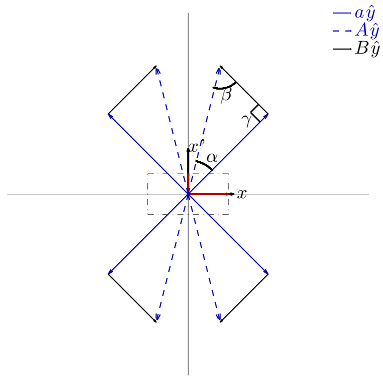

(b) $\hat{y} \in E$ in $\mathbf{M}$

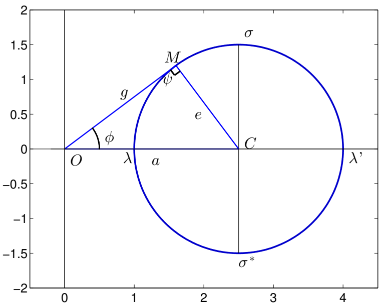

(c) Bireal spectral plane

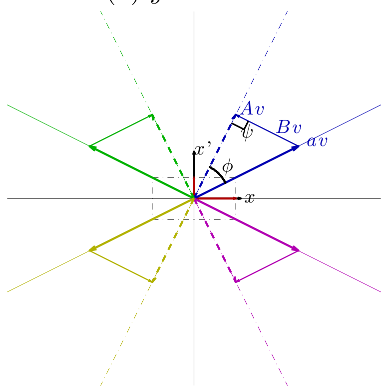

(d) $v \in D_+$ in $\mathbf{M}$

FIGURE 10. $\lambda = 1$, $\lambda' = 4$, $a = 2.5$, $e = 1.5$, $g^2 = 2$, $\cos\phi = 0.8$, $\phi \approx 0.6435$, $\cos\psi = 0$, $\psi = \frac{\pi}{2}$

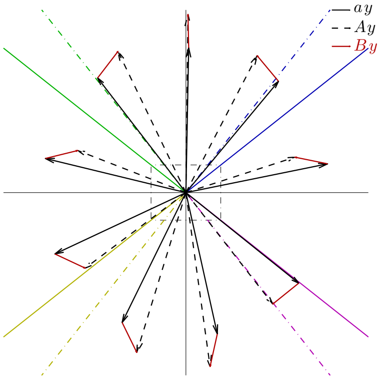

(a) $y \in (C)$, ay, Ay and By in $\mathbf{M}$

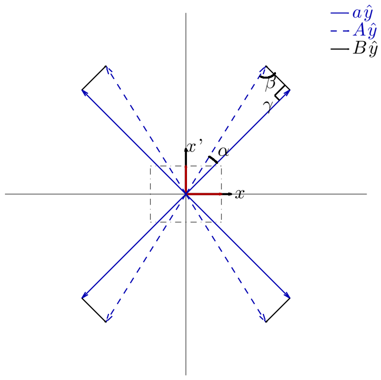

(b) $\hat{y} \in E$ in $\mathbf{M}$

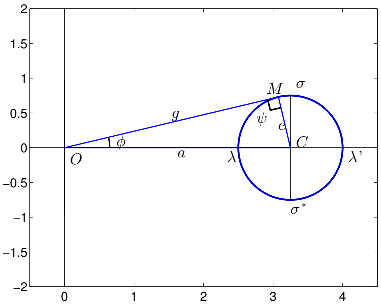

(c) Bireal spectral plane

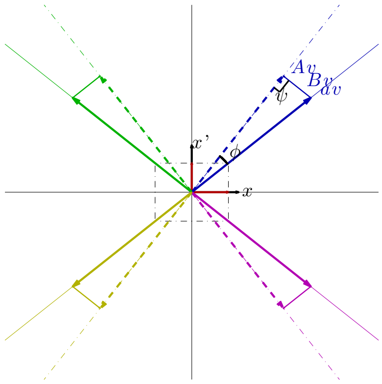

(d) $v \in D_+$ in $\mathbf{M}$

FIGURE 11. $\lambda = 2.5$, $\lambda' = 4$, $a = 3.25$, $e = 0.75$, $g^2 = 10$, $\cos\phi = 0.9730$, $\phi \approx 0.2328$, $\cos\psi = 0$, $\psi = \frac{\pi}{2}$

When $v \in D_-$ (case $g^2 < 0$), we have that: $\|Av\| = |g|$, $\langle v, Av\rangle = 0$, $\langle Bv, Av\rangle = -g^2$, $\cos\phi = 0$ and $\cos\psi = \frac{\langle Bv, Av\rangle}{\|Bv\|\|Av\|} = \frac{|g|}{e}$. See Figure 7 (b) and Figures 12 (c) and 13 (c) for examples. In this case, $v \in D_-$ minimises $|\cos\beta|$ over $\mathbf{M}$ where $\cos\beta$ is the functional

$$0 \neq y \in \mathbb{R}^n \setminus (\text{Ker } A \cup \text{Ker } B) \mapsto \cos\beta(AB, y) = \frac{y^T ABy}{\|By\|\|Ay\|} \tag{4.4}$$

with Euler's equation

$$\frac{A^2 y}{\|Ay\|^2} - 2\frac{ABy}{\langle By, Ay\rangle} + \frac{B^2 y}{\|By\|^2} = 0, \quad 0 \neq y \in \mathbb{R}^n \setminus (\text{Ker } A \cup \text{Ker } B). \tag{4.5}$$

The angle ψ is called the *inner perspective angle* which expresses the inner flexibility of A (i.e. change of perspective, $0 \in [\lambda, \lambda']$). Each self-image Av is orthogonal to v, i.e. the direction of Av differs maximally from that of v, therefore v is called an *antieigenvector*. Two illustrations are given in Figures 12 and 13. According to (4.4) and since $\phi = \frac{\pi}{2}$, the angles $\alpha = \phi = \measuredangle(v, Av)$ and $\beta = \psi = \measuredangle(Bv, Av)$ are extremal (compare (a) and (d)). The right triangles OMC in Figures 12 (c) and 13 (c) are equal to the triangles formed by av, Bv and Av in Figs. 12 (d) and 13 (d).

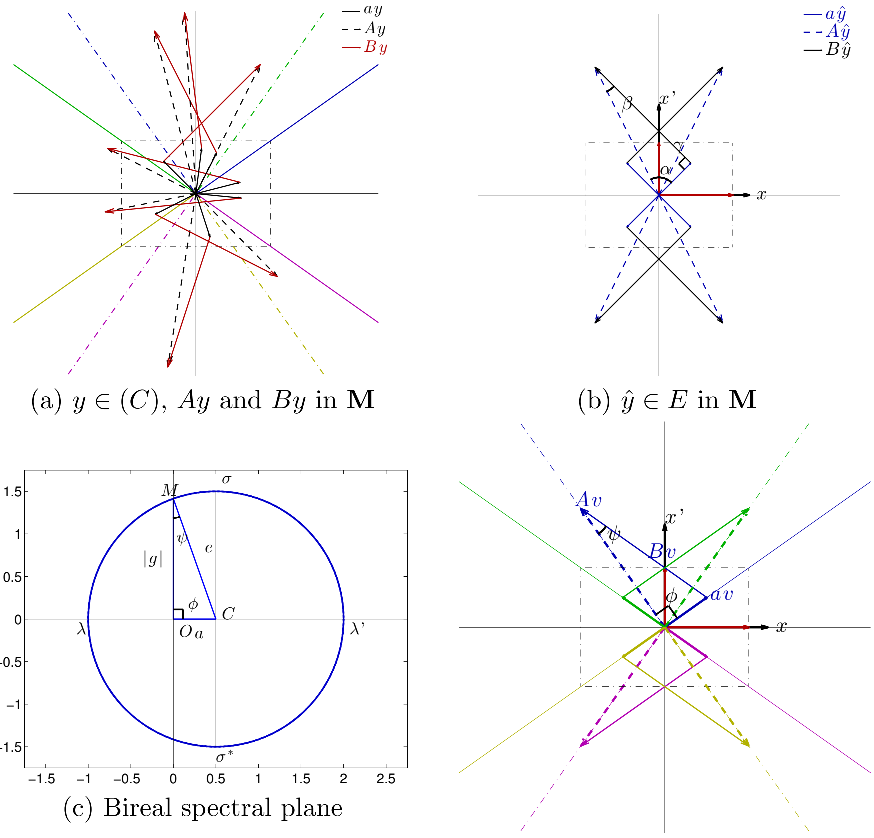

(a) $y \in (C)$, Ay and By in $\mathbf{M}$

(b) $\hat{y} \in E$ in $\mathbf{M}$

(c) Bireal spectral plane

(d) $v \in D_-$ in $\mathbf{M}$

FIGURE 12. $\lambda = -1$, $\lambda' = 2$, $a = 0.5$, $e = 1.5$, $g^2 = -2$, $\cos\phi = 0$, $\phi = \frac{\pi}{2}$, $\cos\psi = 0.9428$, $\psi = 0.3398$

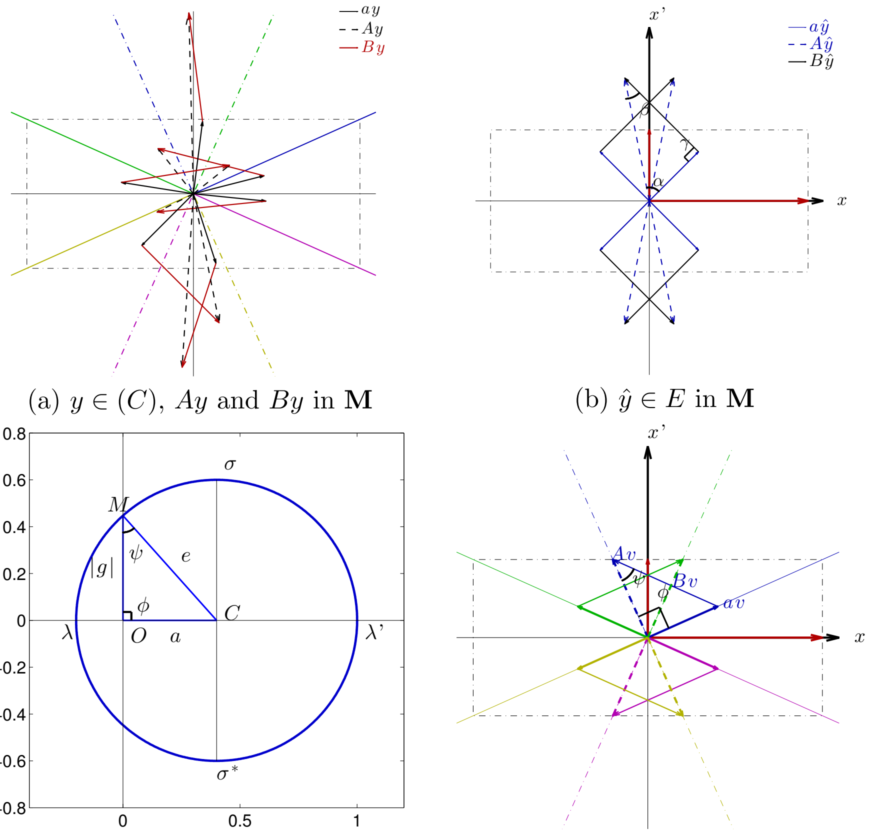

(a) $y \in (C)$, Ay and By in $\mathbf{M}$

(b) $\hat{y} \in E$ in $\mathbf{M}$

(c) Bireal spectral plane

(d) $v \in D_-$ in $\mathbf{M}$

FIGURE 13. $\lambda = -0.2$, $\lambda' = 1$, $a = 0.4$, $e = 0.6$, $g^2 = -0.2$, $\cos\phi = 0$, $\phi = \frac{\pi}{2}$, $\cos\psi = 0.74536$, $\psi = 0.72973$

Historically the functional

$$y \in \mathbb{R}^n \setminus (\{0\} \cup \text{Ker } A) \mapsto \frac{y^T Ay}{\|y\|\ \|Ay\|} = \cos\phi(A, y), \quad \phi(A, y) = \measuredangle(y, Ay),$$

was first considered in [Gustafson, 1968], [Gustafson, 2012] and studied from a standard analytic point of view over $\mathbb{R}$, under the assumption that A is definite. The case $g^2 = \lambda\lambda' < 0$ which may arise when A is indefinite and so far ignored by Gustafson, is treated in [Chatelin, 2016].

If $\lambda = \lambda_{\min}$ and $\lambda' = \lambda_{\max}$ are the smallest and largest eigenvalues of A, then the functionals (4.2) (if $\lambda_{\min}\lambda_{\max} > 0$) and (4.4) (if $\lambda_{\min}\lambda_{\max} < 0$) attain a global minimum, (not only local over $\mathbf{M} = \{x_{\min}, x_{\max}\}$) but over $\mathbb{R}^n$.

Finally the elements in E are such that $\gamma = \measuredangle(y, By) = \frac{\pi}{2}$ and in this case the surface $\frac{1}{2}|a|e\sin\gamma$ of the triangle $\mathbf{T}(y)$ formed by ay, By and Ay (Figure 8 (b)) is maximised: $\mathbf{T}(\hat{y})$ is right-angled ($\sin\gamma = 1$). The four triangles are exemplified in Figures 10 (b) and 11 (b) for $g^2 > 0$ and in Figures 12 (b) and 13 (b) for $g^2 < 0$.

The Euler equations (4.3) and (4.5) can be contrasted with the Euler equation for the Rayleigh quotient $\frac{\langle x, Ax\rangle}{\|x\|^2}$

$$Ax - \frac{\langle x, Ax\rangle}{\|x\|^2}x = 0, \quad x \in \mathbb{R}^n \setminus \{0\}. \tag{4.6}$$

Equations (4.3) and (4.5) indicate that the three vectors x, Ax and A^2x are coplanar whereas in equation (4.6) x and Ax are colinear.

For a more complete optimisation perspective on spectral coupling see [Chatelin and Rincon-Camacho, 2015]. This paper in preparation shows that the optimal information provided by spectral coupling of $\{\lambda, \lambda'\}$ can be interpreted in terms of the two real parameters a and e, derived from $\lambda_\pm = a \pm e \in \mathbb{R}$ and $\sigma_\pm = a \pm ue \in {}^2\mathbb{R}$, to which are associated two distinct measures in the bireal plane: (i) $\sqrt{a^2+e^2}$ = euclidean distance from O to σ or σ^*, and (ii) $|g| = \sqrt{|a^2 - e^2|} = \sqrt{|\text{magnitude}|}$. The optimality is expressed geometrically in $\mathbf{M} \subset \mathbb{R}^n$ by two principles. If one chooses (i), the surface of the triangle $\mathbf{T}(\hat{y})$ is maximal for $\gamma = \frac{\pi}{2} \Leftrightarrow \hat{y} \in E$. On the other hand, the choice (ii) yields $\min|\cos\alpha| > 0$, $\cos\beta = 0$ achieved by catchvectors in D_+ when the magnitude g^2 is > 0 and $\min|\cos\beta| > 0$, $\cos\alpha = 0$ achieved by antieigenvectors in D_- when $g^2 < 0$.

In other words, the *euclidean* choice (i) leads to an optimal *surface* and the *hyperbolic* choice (ii) leads to a pair of maximal *angles* in $]0, \frac{\pi}{2}]$ where $\frac{\pi}{2}$ is achieved by one of the two angles. An illustration of the choice (i) is provided by Nature as the familiar *photosynthesis* phenomenon displayed by plants.

4.4. **Coupling electricity and magnetism.** One cannot overestimate the importance of Maxwell's equations to describe electromagnetic phenomena. Maxwell was convinced by Tait that the noncommutative field of quaternions was well-fitted to express his equations [Maxwell, 1891]. However he did not make full use of the properties of Hamilton's multiplication in 4D. A preliminary work [Chatelin, 2015] confirms that Maxwell's insight was right, and that his vision −when further developped− sheds more light on the electromagnetic potential [Chatelin, 2016] .

5. Two PDE Examples: Δ (elliptic) vs. $\Box$ (hyperbolic)

Two fundamental differential operators in physics are the Laplace operator $\Delta = \frac{\partial^2}{\partial x^2} + \frac{\partial^2}{\partial y^2}$ which defines Laplace's equation $\Delta v = 0$ the archetypal elliptic PDE and the d'Alembert operator $\Box = \frac{\partial^2}{\partial x^2} - \frac{\partial^2}{\partial y^2}$ leading to the wave equation $\Box u = 0$ which is a hyperbolic PDE. It is no coincidence that these equations pop up in analysis over $\mathbb{C}$ and ${}^2\mathbb{R}$ respectively.

5.1. **Cauchy-Riemann conditions over $\mathbb{C}$ and ${}^2\mathbb{R}$.** Let f be a function $f : \mathbb{C} \to \mathbb{C}$, where $f(z) = v(x,y) + iw(x,y)$ and $v, w \in C^2$. A function f is holomorphic iff f satisfy the Cauchy-Riemann (CR) conditions (Summary A.2) which occurs iff v and w are harmonic, i.e. they satisfy Laplace's equation

$$\Delta v = \Delta w = 0.$$

Now, if f is a function defined on the bireal numbers, $f : {}^2\mathbb{R} \to {}^2\mathbb{R}$, where $f(z) = v(x,y) + uv(x,y)$ and $v, w \in C^2$, the generalisation of the (CR) conditions over ${}^2\mathbb{R}$ implies that f is monogenic iff

$$\Box v = \Box w = 0.$$

Nowadays, hyperbolic PDEs are solved with tools (such as complex numbers and finite elements) best suited for elliptic PDEs. We are currently exploring the potential of planar number rings as an alternative to solve hyperbolic or parabolic PDEs.

5.2. **Spectral coupling for the finite difference approximations.** Now, let us apply the results of Section 4.3 to the discrete finite difference versions of the above operators. For Laplace's operator we solve the discrete version of the Dirichlet problem:

$$\begin{cases} -\Delta u &= \lambda u \quad \text{in } \Omega =]0,1[^2, \\ \quad u &= 0 \quad\ \ \text{on } \partial\Omega, \end{cases}$$

with mesh size $h = \frac{1}{N} = 30$. The eigenvalues λ are all negative, the eigenvectors $u_{\min}$ and $u_{\max}$ corresponding to the maximum and minimum eigenvalues $\lambda_{\min}$ and $\lambda_{\max}$ are plotted in Figure 14 (a) and (b) respectively. We couple $\{\lambda_{\min}, \lambda_{\max}\}$; the resulting catchvector u_c is displayed in Figure 14 (c), its image under A the discrete version of Δ is displayed in Figure 14 (d) and its image under $B = A - aI$ ($a = \frac{\lambda_{\min}+\lambda_{\max}}{2}$) is displayed in Figure 14 (e). We are in the case of a definite operator, thus the angle $\phi(A) = \frac{7\pi}{15}$, where $\cos\phi(A) = \frac{\langle u_c, Au_c\rangle}{\|\|u_c\|Au_c\|}$ and in this case we have that $Au_c \perp Bu_c$ ($\psi = \frac{\pi}{2}$).

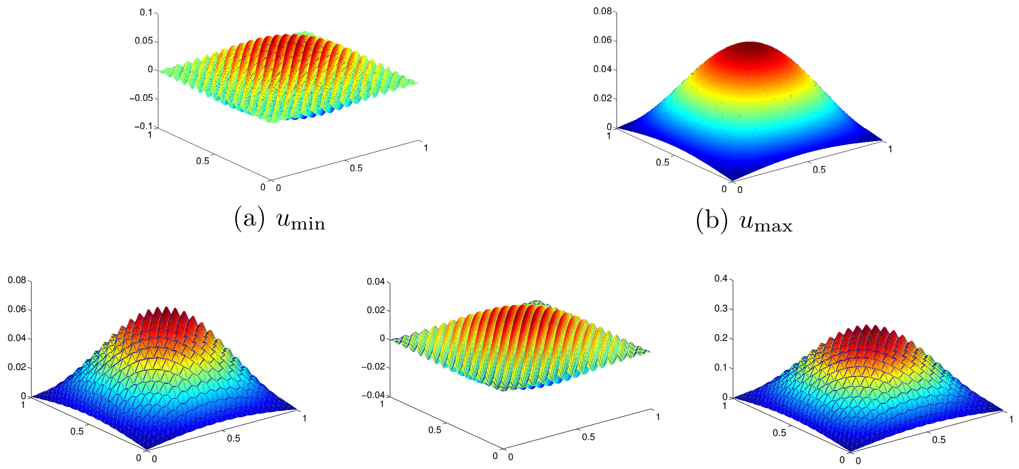

(a) $u_{\min}$ (b) $u_{\max}$

(c) u_c (d) Au_c (e) Bu_c

FIGURE 14. Discrete Laplace operator

The discrete problem to be solved in the case of the d'Alembert operator is:

$$\begin{cases} \Box u &= \lambda u \quad \text{in } \Omega =]0,1[^2, \\ \quad u &= 0 \qquad \text{on } \partial\Omega, \end{cases}$$

with mesh size $h = \frac{1}{N} = 30$. Here we have an indefinite operator, $\lambda_{\max} > 0 > \lambda_{\min}$ and their corresponding eigenvectors $u_{\min}$ and $u_{\max}$ are plotted in Figure 15 (a) and (b) respectively. We couple again $\{\lambda_{\min}, \lambda_{\max}\}$; the antieigenvector u_a is displayed in Figure 15 (c) together with its image Au_a under the discrete version of the d'Alembertian in Figure 15 (d) and its image Bu_a under $B = A - aI$ in Figure 15 (e). In this case: $u_a \perp Au_a$ ($\phi = \frac{\pi}{2}$).

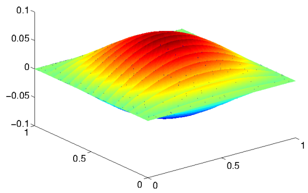

(a) $u_{\min}$

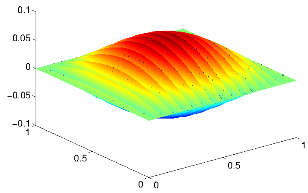

(b) $u_{\max}$

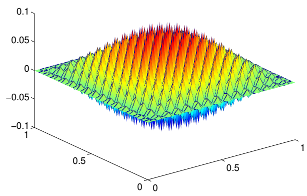

(c) u_a

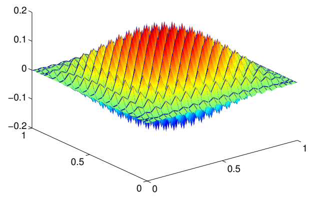

(d) Au_a

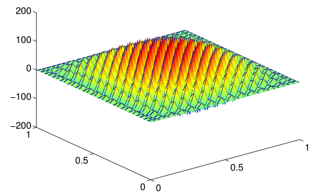

(e) Bu_a

FIGURE 15. Discrete d'Alembert operator

6. Nonlinear computing algebras in Engineering

The nonlinear algebras in which the Qualitative Computing group has been interested are motivated by equations derived from physics in general and by the multi-physic coupling of phenomena in particular.

6.1. **Considerations about dimensions.** One should keep in mind the distinction between the physical dimension of the problem as opposed to its numerical dimension resulting from discretisation. The dimension of the algebras is connected to the physical dimension. For instance in order to perform rotations in the plane, complex numbers are well suited and they are of dimension 2. In order to perform 3D rotations, Hamilton has described how the quaternions $\mathbb{H}$ (of dimension 4) effectively model rotations in $\mathbb{R}^3$. A rigid transformation (the composition of a rotation and a translation, 7D) is well modelled by means of dual quaternions $\mathbb{H}(\mathbb{D})$ (of dimension 8), see [Clifford, 1873, Daniilidis, 1999, Kavan et al., 2008, Pham et al., 2010, Rincon-Camacho and Latre, 2013].

The use of algebraic structures whose dimension appropriately matches the physical problem may lead to more efficient computations, as is often the case in robotics [Dimentberg, 1968].

6.2. **Attractive algorithmic facts.** In order to work with complex numbers, in different computational languages the overloading of operators and functions is used. No more work is required when working with bireal or dual numbers. Moreover, the iterative construction of the algebras (see summary B.2) is reflected into the programming.

For instance, when working with multiplanar numbers described in Section 2.1 or pluridual numbers described in Section 2.2, only the operators (+) and (×) and basic functions need to be overloaded for an algebra of dimension 2 ($\mathbb{C}$, ${}^2\mathbb{R}$, $\mathbb{D}$). When the dimension is increased to 2^k (R_k or $\mathbb{D}^{(k)}$, $k > 1$), the function evaluation is done recursively due to the nested character of these algebras.

Moreover, the use of idempotent vectors when working with mutiplanar numbers, indicates numerically the path to parallelism, when the use of the idempotent basis is adopted.

6.3. **Global classification of nonlinear computing algebras.** In the Annex B.3 on page 28, a global classification is presented for the different algebras studied by the QC group with Computation in mind. This table allows us to compare the structures therein. A description of various effective uses of algebras of dimension 2, 4 and 8 in Science and Technology can be found in [Latre, 2013]. In Table 1 below some of these applications are listed, using the following numbering:

1:	Signal Processing	6:	Special Relativity
2:	Image Processing	7:	Quantum Mechanics
3:	Kinematics	8:	High Energy Physics
4:	Robotics	9:	Differentiation/Optimisation
5:	Electromagnetism	10:	Hydrodynamics

dimension	algebras				
2	$\mathbb{C}$	$\cancel{\mathbb{C}} \equiv {}^2\mathbb{R}$ 1, 2, 6,10		$\mathbb{D}$ 1, 2, 4, 9	
4	$\mathbb{H}$ 1, 2, 5, 7	$\cancel{\mathbb{H}}$ 5, 6	${}^2\mathbb{C} = \mathbb{C}({}^2\mathbb{R})$ 1, 2, 5, 7	$\mathbb{C}(\mathbb{D})$ 1, 2, 4	$\mathbb{D}(\mathbb{D})$ 9
8	$\mathbb{G}$ 3, 5, 7	$\cancel{\mathbb{G}}$ 5,7	${}^2\mathbb{H} = \mathbb{H}({}^2\mathbb{R})$ 3	$\mathbb{H}(\mathbb{D})$ 1, 2, 4	$\mathbb{H}(\mathbb{C})$ 5,6,7,8

TABLE 1. Nonlinear computing algebras in Science and Tecnology

The importance of the unipotent unit u resurfaced only at the end of the 20^{th} century [Price, 1991, Sobczyk, 1995]. By comparison, the nilpotent unit n was slightly more successful.

After their discovery in the 19^{th} century by Clifford, dual numbers $\mathbb{D}$ and dual quaternions $\mathbb{H}(\mathbb{D})$ quickly found a natural application in the specific domain of rigid body dynamics with the seminal works of [Kotelnikov, 1895] and [Study, 1903], who introduced the principle of transference (= equivalence between dual and classic equations). These first works have been continued during the 20^{th} century especially by the russian school of mechanics [Dimentberg, 1948, Dimentberg, 1968], which inspired further developments [Yang and Freudenstein, 1964, Veldkamp, 1976]. This research topic remains extremely active today in kinematics [Cheng and Thompson, 1996, Pennestrì and Stefanelli, 2007].

On the engineering side, duals and dual quaternions have become most popular number tools in robotics [Daniilidis, 1999] and computer graphics [Kavan et al., 2008].

Various authors have highlighted their many technical advantages: (i) compact formulation (=reduction of the number of equations), (ii) accurate treatment of singularities, both at theoretical and numerical levels, and (iii) extremely efficient behaviour regarding numerical resolution. According to some authors, dual numbers and dual quaternions provide for mechanics of rigid bodies the *optimal representation* in terms of significant parameters: they are not plagued with the *redundancies* present in standard matrix techniques.

In most other domains, the situation is not so advanced and calls for much more work. In general, the applications of the computing algebraic structures which are found in the literature are independent from one another. By taking a global view on these algebras, the research conducted by the QC group looks for mathematical justifications underlying the optimal use of a certain kind of algebra for a certain physical problem.

For example, there exist in the literature at least 4 different representations in 8 dimensions of the electromagnetic field and the corresponding Maxwell equations:

• in $\mathbb{H}(\mathbb{C})$ (complex quaternions), [Alexeyeva, 2009, Alexeyeva, 2012, Kassandrov, 2000, Kassandrov, 2007, Kravchenko, 2003, Christianto, 2010, Kansu et al., 2012, Girard, 1984, van Vlaenderen and Waser, 2001],
• in $\mathbb{H}(\mathbb{D})$ (dual quaternions), [Demir and Ozdas, 2003],
• in $\mathbb{G}$ (octonions), [Bisht et al., 2007],
• in $\not{\mathbb{G}}$ (split-octonions), [Bisht et al., 2007, Chanyal et al., 2011, Candemir et al., 2008, Nurowski, 2009].

This raises the obvious question: which representation is the best relatively to a prescribed goal? Given the currently underexploited mathematical wealth of the 4 algebras above, to risk an answer today would be premature. However, the work [Chatelin, 2015] indicates that a purely 4D-evolution in $\mathbb{H}$ of the coupled electric and magnetic fields reveal new aspects of the electromagnetic potential, a fact which could, in turn, suggest more efficient resolution methods.

7. Conclusions

The better part of the activity of the QC group during the past two years has been devoted to bibliographic researches. The literature on nonstandard algebras which are suited for computation is rare, scattered between several domains from Mathematics and Physics to Engineering; moreover its time span covers at least 170 years (starting with the invention of quaternions and octonions in 1843).

To the best of our knowledge, our research represents the first comprehensive effort to survey Computing Algebras (beyond the popular linear algebra of square matrices) that has been undertaken since Cartan's encyclopedic paper about hypercomplex numbers in 1908.

During our classification work, we have found here and there new theoretical results reported in [Chatelin, 2016]. After our purely quaternionic treatment of electromagnetism [Chatelin, 2015, 2016], the second most promising of our advances to-date concerns spectral coupling in the spectral theory of symmetric matrices (Section 4.3 above). This novel dynamic perspective on a classical static problem offers new mathematical tools to think about *self-organisation* in natural phenomena. To this date, our work has uncovered more questions about computation than it has been able to solve...

To further our understanding of the autonomous dynamics of computation, we have started a new line of investigation which addresses, beyond boolean logic, the evolution of computational logics under the pressure of nonlinear computation. It is centered on the analytic multiplication represented by the composition $f \circ g = f(g(\cdot))$ of 2 continuous functions f, g in $C^0(\mathbb{R})$. [Rincon-Camacho et al., 2014a, 2014b, 2014c]. The results will be presented in the next activity report.

Acknowledgement The authors are grateful for the financial support from the Scientific Direction TOTAL through the contract DS-2755-B with Cerfacs (Qualitative Computing group).

Technical Annex

Here we present a very limited overview of the nonlinear computing algebras studied by the group.

A. 2D Algebras

A.1. **A threefold algebraic structure for the number plane** $\mathbb{R} \times \mathbb{R}$. Let α, $\beta \in \mathbb{R}$, then the real algebra $\mathcal{A}(\alpha, \beta) = \mathcal{A}$ is defined by two multiplicative generators: the real unit 1 and the non real unit g such that

$$g^2 = \alpha + 2\beta g, \quad \alpha, \beta \in \mathbb{R}.$$

For two elements $z_1 = x_1 + y_1 g$ and $z_2 = x_2 + y_2 g$ in $\mathcal{A}$, the addition, the scalar multiplication and the multiplication are as follows:

- $z_1 + z_2 = (x_1 + x_2) + (y_1 + y_2)g$,
- $sz = \tau x + syg$, $s \in \mathbb{R}$
- $z_1 z_2 = (x_1 x_2 + \alpha y_1 y_2) + (x_1 y_2 + x_2 y_1 + 2\beta y_1 y_2)g$.

The conjugation given by $g^* = 2\beta - g$ and $z^* = x + yg^* = x + 2\beta y - yg$ allow us to define the *magnitude*

$$\begin{aligned}
\mu(z) &= zz^* \\
&= x^2 + 2\beta xy - \alpha y^2 \\
&= (x + \beta y)^2 - (\alpha + \beta^2)y^2 \\
&= z^T S z, \quad S = \begin{pmatrix} 1 & \beta \\ \beta & -\alpha \end{pmatrix}, \quad z = \begin{pmatrix} x \\ y \end{pmatrix}.
\end{aligned}$$

The nature of the *quadratic* form $\mu(z)$ is given by the sign of $\delta = \alpha + \beta^2 = -\det S$ which defines three types of structure for $\mathcal{A}$:

i. *elliptic* numbers for $\delta < 0$, which form a field and $(\mu(z))^{\frac{1}{2}} = \|z\|_S = \|S^{\frac{1}{2}} z\|_2$ is a norm,
ii. *parabolic* numbers for $\delta = 0$, a ring with zerodivisors and $(\mu(z))^{\frac{1}{2}}$ a semi-norm,
iii. *hyperbolic* numbers for $\delta > 0$, a ring with zerodivisors and $\mu(z) \in \mathbb{R}$ has no definite sign.

In case iii., $\mu(z)$, when > 0, satisfies a reverse Cauchy inequality. In Special Relativity in 1 space variable, the indefinite sign of $\mu(z)$ leads to the distinction between space-like and time-like distances.

In Figure 16 the parabola $\alpha = -\beta^2 \Leftrightarrow \delta = 0$ is the border in the eidetic plane (α, β) which separates all (α, β) leading to elliptic numbers from all those leading to hyperbolic numbers in $\mathcal{A}(\alpha, \beta)$.

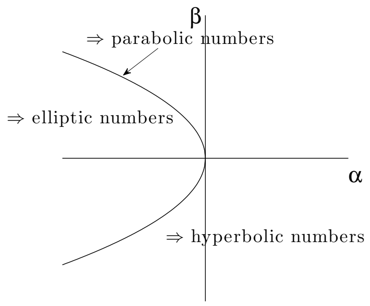

FIGURE 16. In the eidetic plane $(\alpha, \beta) \in \mathbb{R}^2$ $\delta = \alpha + \beta^2 < 0, \quad = 0, \quad > 0$

The three canonic cases complex, dual and bireal are given by $\beta = 0$, $g^2 = \alpha \in \{-1, 0, 1\}$, [Yaglom, 1968, Kantor and Solodovnikov, 1989].

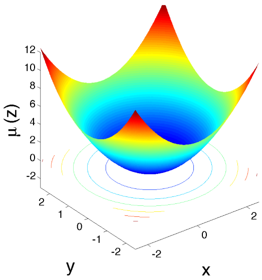

FIGURE 17. $\mathbb{C}$: $\mu(z) = x^2 + y^2$

Complex numbers $\mathbb{C}$: The classical and well studied example of elliptic numbers are the complex numbers $\mathbb{C}$, given by $\alpha = -1$, $\beta = 0$. Here $g = i = \sqrt{-1}$ is called the *imaginary* unit ($i^2 = -1$). Thus, $\mathbb{C} = \mathbb{R} \oplus i\mathbb{R}$, $z = x + iy$, $\bar{z} = z^* = z - iy$ and $\mu(z) = zz^* = x^2 + y^2$. In this case $(\mu(z))^{\frac{1}{2}} = \sqrt{x^2 + y^2}$ is the modulus $|z|$ which is the euclidean norm of $\vec{z} = (x, y) \in \mathbb{R}^2$.

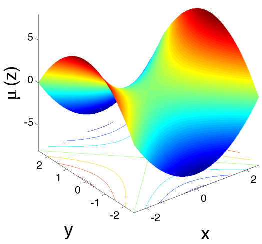

FIGURE 18. ${}^2\mathbb{R}$: $\mu(z) = x^2 - y^2$

Bireal numbers ${}^2\mathbb{R}$: If $\alpha = 1$, $\beta = 0$, $g = u$, we obtain the bireal numbers introduced by [Cockle, 1848] which are of hyperbolic type. Here $u^2 = 1$ provides the *unipotent* unit, $u = \sqrt{1}$, $u \neq \pm 1$, ${}^2\mathbb{R} = \mathbb{R} \oplus \mathbb{R}u$, $z = x + yu \in {}^2\mathbb{R}$ and $\mu(z) = x^2 - y^2$, thus $\mu(z) \in \mathbb{R}$ can be positive, negative or zero.

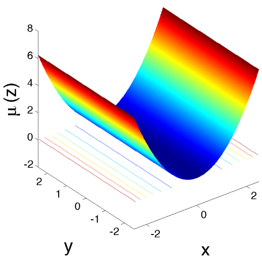

FIGURE 19. $\mathbb{D}$: $\mu(z) = x^2$

Dual numbers $\mathbb{D}$: The dual numbers $\mathbb{D}$ studied in [Clifford, 1873] are given by $\alpha = \beta = 0$ and they have a parabolic nature. Here $g = n = \sqrt{0}$, $n \neq 0$, is a *nilpotent* unit, $n^2 = 0$, $\mathbb{D} = \mathbb{R} \oplus \mathbb{R}n$ and $\mu(z) = x^2$, $z = x + yn \in \mathbb{D}$. Thus $(\mu(z))^{\frac{1}{2}} = |x|$ defines a semi-norm.

There exists an isomorphism between $\mathcal{A}(\alpha, \beta)$ and $\mathcal{A}(\pm 1, 0)$ and between $\mathcal{A}(-\beta^2, \beta)$ (i.e. $\delta = 0$) and $\mathcal{A}(0, 0)$. A description of these quadratic algebras is given in [Chatelin, 2016, chapter 2].

Example 1: A compelling example about the differences between the three types of numbers (elliptic, parabolic and hyperbolic) is the quadratic iteration $z \mapsto z^2 + c$ and its dynamics in the plane. When $z \in \mathbb{C}$: complex dynamics leads to the well-known Mandelbrot set, when $z \in {}^2\mathbb{R}$: bireal dynamics leads to a square, and when $z \in \mathbb{D}$: dual dynamics leads to a vertical strip; all three sets are based on $[-2, \frac{1}{4}]$ horizontally. See Figure 20.

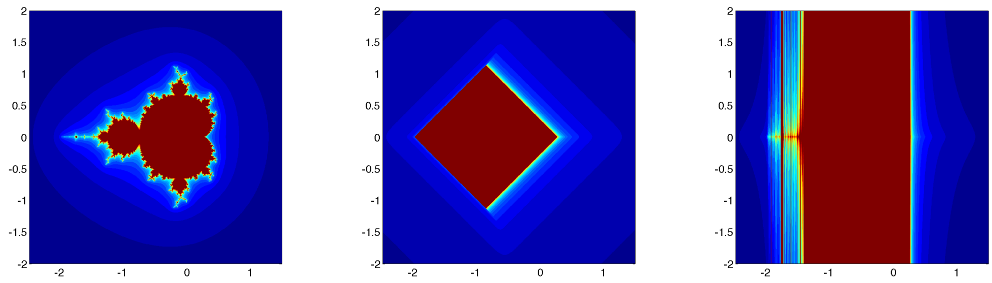

(a) $z \in \mathbb{C}$ (b) $z \in {}^2\mathbb{R}$ (c) $z \in \mathbb{D}$

FIGURE 20. Quadratic iteration $z \mapsto z^2 + c$

A.2. **Analysis in the numerical plane.** Let f be a function, $f : \mathcal{A}(\alpha, \beta) \to \mathcal{A}(\alpha, \beta)$, where $f(z) = v(x, y) + w(x, y)g,\ v, w \in C^1$. The directional derivative of f at z in the direction $\xi = 1 + pg$ with slope p is as follows

$$f'(z, \xi) = \frac{v_x + w_x g + p(v_y + w_y g)}{1 + pg}$$

where $\xi \neq 0$ at it is not a zerodivisor. Then, $f'(z, \xi)$ may be written in the form

$$f'(z, \xi) = X + Yg,$$

where X and Y depend on v_x, v_y, w_x, w_y and possibly on p. X and Y are independent of p when the following generalised Cauchy-Riemann (CR) conditions in $\mathcal{A}(\alpha, \beta)$ are satisfied:

$$v_x = w_y - 2\beta w_x, \quad v_y = \alpha w_x. \tag{A.1}$$

In this case f is called *monogenic*, otherwise f is polygenic [Kasner, 1927]. When X and Y are dependent on p, they satisfy the following quadratic equation

$$X^2 - \alpha Y^2 + 2\beta XY - X(v_x + w_y) + Y(v_y - 2\beta v_x + \alpha w_x) + v_x w_y - v_y w_x = 0, \tag{A.2}$$

which is called the *derivative conic* [Capelli, 1941]. In the case of the complex numbers $\mathbb{C}$, ($\alpha = -1$, $\beta = 0$) (A.2) becomes a circle, for the bireal numbers ${}^2\mathbb{R}$ ($\alpha = 1$, $\beta = 0$) (A.2) is an hyperbola and for the dual numbers $\mathbb{D}$, ($\alpha = 0, \beta = 0$) (A.2) is a parabola. For more about the analysis in the numerical plane, see [Chatelin, 2016, chapter 4].

Example 2: Real functions $f : \mathbb{R} \to \mathbb{R}$, such as sin, cos, exp or polynomials among others can be extended to complex, dual or bireal functions, see [Chatelin, 2016, chapter 2]. For example the sinus function is extended as follows:

$$\begin{aligned}
&f_1 : \quad \mathbb{C} \to \mathbb{C}, && f_1(z) = \sin(x + iy) = \sin x \cosh y + i \cos x \sinh y,\\
&f_2 : \quad {}^2\mathbb{R} \to {}^2\mathbb{R}, && f_2(z) = \sin(x + uy) = \sin x \cos y + u \cos x \sin y,\\
&f_3 : \quad \mathbb{D} \to \mathbb{D}, && f_3(z) = \sin(x + ny) = \sin x + n(\cos x)y.
\end{aligned} \tag{A.3}$$

Each function f_1, f_2 and f_3 satisfies the (CR)-conditions (A.1).

Example 3: Euler's formula $e^{i\theta} = \cos\theta + i \sin\theta$ extends to the bireal and dual numbers as follows:

$$e^{u\theta} = \cosh\theta + u \sinh\theta \ \text{ over } {}^2\mathbb{R}, \ \text{ and } \ e^{n\theta} = 1 + n\theta \ \text{ over } \mathbb{D}.$$

In Figure 21 the three curves defined by $e^{i\theta}$, $e^{u\theta}$ and $e^{n\theta}$ are displayed for $\theta \in [0, 2\pi[$, or $\theta \in \mathbb{R}$. We note that $\mu(e^{i\theta}) = \mu(e^{u\theta}) = \mu(e^{n\theta}) = 1$ and that 1 is a triple point.

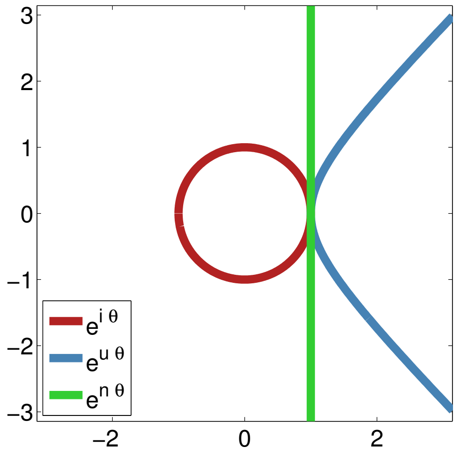

FIGURE 21. Euler's formulae in $\mathbb{C}$, ${}^2\mathbb{R}$ and $\mathbb{D}$

B. Algebraic constructions

B.1. **General construction.** There are different ways in which hypercomplex numbers in any dimension n can be constructed. Let K be equal to $\mathbb{R}$ or $\mathbb{C}$, then the linear vector space K^n, $n \geq 3$ with basis $\{e_i\}$, $i = 1$ to n can be transformed into an algebra by defining the multiplication

$$e_i \times e_j = \sum_{k=1}^{n} \gamma_{ijk} e_k, \quad 1 \leq i, j, \leq n$$

which is distributive with respect to addition, we denote this algebra by $\mathcal{K}$. The *structural cube* is formed by the n^3 scalars $\gamma_{ijk} \in K$ and is represented in Figure 22.

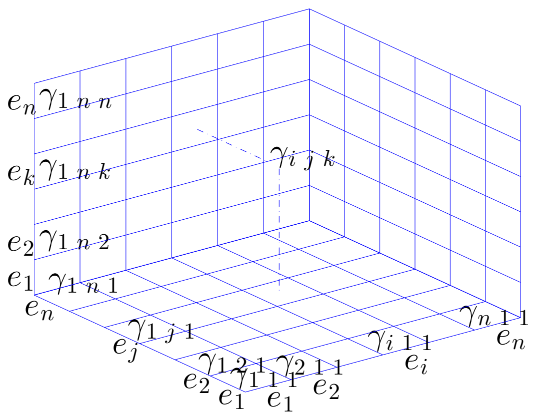

FIGURE 22. Structural cube $\gamma_{ijk} \in K$

The associativity property $((e_i \times e_j) \times e_l = e_i \times (e_j \times e_l))$ is guaranteed iff the scalars $\gamma_{ijk} \in K$ satisfy the condition

$$\sum_{k=1}^{n} \gamma_{ijk}\gamma_{klm} = \sum_{k=1}^{n} \gamma_{ikm}\gamma_{jlk}, \quad 2 \leq i, j, k \leq n, \quad 1 \leq m \leq n.$$

The algebra of hypercomplex numbers which is associative is denoted by $\mathcal{K}_a$. The commutativity condition $e_i \times e_j = e_j \times e_i$ is satisfied iff

$$\gamma_{ijk} = \gamma_{jik}, \quad 1 \leq i, j, k \leq n.$$

If the hypercomplex algebra is associative and commutative, it consists of *analytic numbers* and is denoted by AN_n because the classical differential and integral calculus may be performed [Scheffers, 1893]. For more information about the hypercomplex numbers see [Chatelin, 2016, chapter 7].

B.2. **Iterative construction.** Hypercomplex algebras may also be constructed in an iterative way. For example, the Dickson algebra sequence $A_k \cong \mathbb{R}^{2^k}$, $A_0 = \mathbb{R}$, $k \geq 0$ is constructed by a duplication process

$$A_{k+1} = A_k \oplus A_k \times \tilde{1}, \quad k \geq 0,$$
$$z = x + y\tilde{1}, \quad x, y \in A_k, \quad \tilde{1}^2 = -1, \quad \tilde{1} = (0,1) \notin A_k$$

where the conjugation and multiplication are defined recursively:

$$\overline{(x,y)} = (\bar{x}, -y)$$

$$(x,y) \times (x',y') = (x \times x' - \bar{y}' \times y, y' \times x + y \times \bar{x}') \tag{B.1}$$

Thus, $A_1 = \mathbb{C}$ (a commutative field) and $A_2 = \mathbb{H} = \{\text{quaternions}\}$ (a noncommutative field), $A_3 = \mathbb{G} = \{\text{octonions}\}$ (a nonassociative division algebra) see [Chatelin, 2012b].

If in (B.1) the $-$ sign is replaced by $+$ we get the split-Dickson algebra family $\cancel{A}_k$ because the Dickson magnitude = squared euclidean norm = $\|x\|^2 = \sum_1^{2^k} x_i^2$ is "split" as $\sum_{i=1}^{2^{k-1}} x_i^2 - \sum_{j=2^{k-1}+1}^{2^k} x_j^2$. For example, the bireal algebra $\cancel{A}_1 =^2 \mathbb{R}$ is the algebra $\cancel{\mathbb{C}}$ of split-complexes.

Two other examples of numbers iteratively constructed are the multiplanar numbers defined in Section 2.1 and pluridual numbers defined in Section 2.2.

B.3. **Nonstandard computing algebras.** The following table contains the computing algebras studied by the Qualitative Computing group. The algebras whose multiplication is commutative and associative, are coloured in red, in green the ones with associative multiplication and in blue the ones with non associative multiplication.

dimension	algebras		
$n \geq 3$	$\mathcal{K}$ arbitrary hypercomplex numbers	$\mathcal{K}_a$ associative hypercomplex numbers	AN_n analytic numbers (associative and commutative hypercomplex numbers)

$n = 2^k$											
	1 $k=0$	$\mathbb{R}$ reals									
	2 $k=1$	$\mathbb{D} = \mathcal{A}_0$ duals		$\mathbb{C} = \mathcal{A}_{-1}$ complexes		$\not{\mathbb{C}}$ split complexes	$\cong$	${}^2\mathbb{R} = \mathcal{A}_1$ bireals	planar		
	4 $k=2$	$\mathbb{D}^{(2)} = \mathbb{D}(\mathbb{D})$ double duals	$\mathbb{C}(\mathbb{D}) = \mathbb{D}(\mathbb{C})$ dual complexes	$\mathbb{H}$ quaternions		$\not{\mathbb{H}}$ split quaternions		$\mathbb{C}({}^2\mathbb{R}) = {}^2\mathbb{C} = {}^2\mathbb{R}(\mathbb{C})$ bicomplexes		${}^2\mathbb{R}({}^2\mathbb{R}) = {}^4\mathbb{R}$ quadrireals	${}^2\mathbb{R}(\mathbb{D}) = {}^2\mathbb{D}$ biduals
	8 $k=3$	$\mathbb{D}^{(3)}$ triple duals	$\mathbb{H}(\mathbb{D})$ dual quaternions	$\mathbb{G}$ octonions	$\mathbb{H}(\mathbb{C})$ complex quaternions	$\not{\mathbb{G}}$ split octonions	$\not{\mathbb{H}}(\mathcal{A}_\alpha)$ dual/complex/bireals split quaternions	$\mathbb{H}({}^2\mathbb{R}) = {}^2\mathbb{H}$ bireal quaternions biquaternions	${}^2\mathbb{R}({}^2\mathbb{C}) = {}^4\mathbb{C}$	${}^2\mathbb{R}({}^4\mathbb{R}) = {}^8\mathbb{R}$	${}^2\mathbb{R}({}^2\mathbb{D}) = {}^4\mathbb{D}$
	2^k, $k \geq 4$	$\mathbb{D}^{(k)}$ pluriduals	$A_{k-1}(\mathbb{D})$ dual Dickson	A_k Dickson algebras	$A_{k-1}(\mathbb{C})$ complex Dickson	$\not{A}_k$ split Dickson	$\not{A}_{k-1}(\mathcal{A}_\alpha)$ dual/complex/bireals split Dickson	$A_{k-1}({}^2\mathbb{R}) = {}^2A_{k-1}$ bi-Dickson	$C_k = {}^{2^{k-1}}\mathbb{C}$ multicomplexes	$B_k = {}^{2^k}\mathbb{R}$ multireals	$D_k = {}^{2^{k-1}}\mathbb{D}$ multiduals
									multiplanar		

× non associative
× associative
× commutative and associative

References

[Alexeyeva, 2009] Alexeyeva, L. (2009). Newton's laws for a biquaternionic model of the electro-gravimagnetic field, charges, currents, and their interactions. *Journal of Physical Mathematics*, 1.

[Alexeyeva, 2012] Alexeyeva, L. (2012). Biquaternions algebra and its applications by solving of some theoretical physics equations. *Int. J. Clifford Analysis, Clifford Algebras and their Applications*, 7:19.

[Baez, 2002] Baez, J. (2002). The octonions. *Bulletin of the American Mathematical Society*, 39(2):145–205.

[Bisht et al., 2007] Bisht, P., Pandey, B., and Negi, O. (2007). Interpretations of octonion wave equations. *arXiv preprint arXiv:0708.1664*.

[Braconnier et al., 1995] Braconnier, T., Chatelin, F., and Dunyach, J. (1995). Highly nonnormal eigenproblems in the aeronautical industry. *Japan journal of industrial and applied mathematics*, 12(1):123–136.

[Brodsky and Shoham, 1999] Brodsky, V. and Shoham, M. (1999). Dual numbers representation of rigid body dynamics. *Mechanism and machine theory*, 34(5):693–718.

[Candemir et al., 2008] Candemir, N., Tanisli, M., Ozdas, K., and Demir, S. (2008). Hyperbolic octonionic proca-Maxwell equations. *Zeitschrift fur Naturforschung A-Journal of Physical Sciences*, 63(1-2):15–18.

[Capelli, 1941] Capelli, P. F. (1941). Sur le nombre complexe binaire. *Bulletin of the American Mathematical Society*, 47(8):585–595.

[Cartan, 1908] Cartan, E. (1908). Nombres complexes. in *Encycl. Sc. Math.,* (J. Molk ed.) d'après l'article allemand de Study, I(1-5):329–468 (Gauthier–Villars, Paris).

[Chaitin-Chatelin and Frayssé, 1996] Chaitin-Chatelin, F. and Frayssé, V. (1996). *Lectures on finite precision computations*, volume 1. SIAM.

[Chaitin-Chatelin and Van Gijzen, 2006] Chaitin-Chatelin, F. and Van Gijzen, M. (2006). Analysis of parameterized quadratic eigenvalue problems in computational acoustics with homotopic deviation theory. *Numerical Linear Algebra with Applications*, 13(6):487–512.

[Chanyal et al., 2011] Chanyal, B., Bisht, P., and Negi, O. (2011). Generalized split-octonion electrodynamics. *International Journal of Theoretical Physics*, 50(6):1919–1926.

[Chatelin, 2012a] Chatelin, F. (2012a). *Eigenvalues of Matrices: Revised Edition*, volume 71. SIAM.

[Chatelin, 2012b] Chatelin, F. (2012b). *Qualitative Computing: a computational journey into nonlinearity.* World Scientific, Singapore.

[Chatelin, 2015] Chatelin, F. (2015). Continuous Information Processing in the light of quaternions. *(in preparation).*

[Chatelin, 2016] Chatelin, F. (2016). *Numbers in Mind: The transformative dynamics of Numerics (livre en prparation).* World Scientific and Imperial College Press, London.

[Chatelin and Rincon-Camacho, 2015] Chatelin, F. and Rincon-Camacho, M. M. (2015). Symmetric matrices: Spectral couplings, plane geometry and optimisation. *(in preparation).*

[Cheng and Thompson, 1996] Cheng, H. and Thompson, S. (1996). Dual Polynomials and Complex Dual Numbers for Analysis of Spatial Mechanism. In *Proc. of ASME 24th. Biennial Mechanisms Conference, Irvine, California*, pages 19–22.

[Christianto, 2010] Christianto, V. (2010). A derivation of Maxwell equations in quaternion space. *Progress in Physics, no. 2, april 2010*, 2010(2):23–27.

[Clifford, 1873] Clifford, W. K. (1873). Preliminary sketch of bi-quaternions. *Proc. London Math. Soc*, 4(381-395):157.

[Cockle, 1848] Cockle, J. (1848). III. On Certain Functions Resembling Quaternions, and on a New Imaginary Algebra. *Phil. Mag. (3)*, 33:435–439.

[Daniilidis, 1999] Daniilidis, K. (1999). Hand-eye calibration using dual quaternions. *The International Journal of Robotics Research*, 18(3):286–298.

[Demir and Ozdas, 2003] Demir, S. and Ozdas, K. (2003). Dual quaternionic reformulation of electromagnetism. *Acta Physica Slovaca*, 53(6):429–436.

[Dimentberg, 1948] Dimentberg, F. (1948). A general method for the investigation of finite displacements of spatial mechanisms and certain cases of passive joints. *Akad. Nauk. SSSR Trudi Sem. Teorii Mash. Mekh. (in Russian)*, 5(17):5–39.

[Dimentberg, 1965] Dimentberg, F. (1965). The screw calculus. *(Book in Russian).*

[Dimentberg, 1968] Dimentberg, F. M. e. (1968). The screw calculus and its applications in mechanics. Technical report, DTIC Document (english translation of 1965 book).

[Fike, 2013] Fike, J. A. (2013). *Multi-objective optimization using hyper-dual numbers.* PhD thesis, Stanford University.

[Girard, 1984] Girard, P. (1984). The quaternion group and modern physics. *European Journal of Physics*, 5(1):25.

[Gustafson, 1968] Gustafson, K. (1968). A min-max theorem. *Notices Amer. Math. Soc*, 15:799.

[Gustafson, 2012] Gustafson, K. (2012). *Antieigenvalue Analysis: With Applications to Numerical Analysis, Wavelets, Statistics, Quantum Mechanics, Finance, and Optimization.* World Scientific , Singapour.

[Kansu et al., 2012] Kansu, M. E., Tanisli, M., and Demir, S. (2012). Electromagnetic energy conservation with complex octonions. *Turk J Phys*, 1:8.

[Kantor and Solodovnikov, 1989] Kantor, I. L. and Solodovnikov, A. S. (1989). *Hypercomplex numbers: an elementary introduction to algebras.* Springer Berlin.

[Kasner, 1927] Kasner, E. (1927). A New Theory of Polygenic (or Non-Monogenic) Functions. *Science*, 66(1720):581–582.

[Kassandrov, 2000] Kassandrov, V. (2000). Biquaternion electrodynamics and Weyl-Cartan geometry of space-time. *arXiv preprint gr-qc/0007027.*

[Kassandrov, 2007] Kassandrov, V. V. (2007). Quaternionic Analysis and the Algebrodynamics. *arXiv preprint arXiv:0710.2895.*

[Kavan et al., 2008] Kavan, L., Collins, S., Žára, J., and O'Sullivan, C. (2008). Geometric skinning with approximate dual quaternion blending. *ACM Transactions on Graphics (TOG)*, 27(4):105.

[Kerner, 1986] Kerner, W. (1986). Computing the complex eigenvalue spectrum for resistive magnetohydrodynamics. *North-Holland Mathematics Studies*, 127:241–265.

[Kerner, 1989] Kerner, W. (1989). Large-scale complex eigenvalue problems. *Journal of Computational Physics*, 85(1):1–85.

[Kotelnikov, 1895] Kotelnikov, A. (1895). Screw calculus and some of its applications to geometry and mechanics. *Annals of Imperial University of Kazan.*

[Kravchenko, 2003] Kravchenko, V. V. (2003). *Applied quaternionic analysis*, volume 28. Heldermann.

[Lam, 1999] Lam, T. (1999). *Lectures on Modules and Rings.* Graduate Texts in Mathematics. Springer New York.

[Lantoine et al., 2012] Lantoine, G., Russell, R. P., and Dargent, T. (2012). Using multicomplex variables for automatic computation of high-order derivatives. *ACM Transactions on Mathematical Software (TOMS)*, 38(3):16.

[Latre, 2013] Latre, J. B. (2013). Sur quelques structures algébriques utiles au traitement de l'information en robotique, informatique et physique. *Rapport de Master, 25/03/13-06/09/13, WN-PA-13-105.*

[Martins et al., 2003] Martins, J. R., Sturdza, P., and Alonso, J. J. (2003). The complex-step derivative approximation. *ACM Transactions on Mathematical Software (TOMS)*, 29(3):245–262.

[Maxwell, 1870] Maxwell, J. C. (1870). On the application of the ideas of the calculus of quaternions to electromagnetic phenomena. *Maxwell's Scientific Papers* (Sir W. Niven ed.), 2:570–576, Dover Publ. New York (1890).

[Maxwell, 1891] Maxwell, J. C. (1891). *A treatise on electricity and magnetism.* 3^{rd} edition (J.J. Thomson ed.), Dover republication (1954).

[Nurowski, 2009] Nurowski, P. (2009). Split octonions and Maxwell equations. *Acta Physica Polonica A*, 116.

[Pennestrì and Stefanelli, 2007] Pennestrì, E. and Stefanelli, R. (2007). Linear algebra and numerical algorithms using dual numbers. *Multibody System Dynamics*, 18(3):323–344.

[Pham et al., 2010] Pham, H.-L., Perdereau, V., Adorno, B. V., and Fraisse, P. (2010). Position and orientation control of robot manipulators using dual quaternion feedback. In *Intelligent Robots and Systems (IROS), 2010 IEEE/RSJ International Conference on*, pages 658–663. IEEE.

[Piponi, 2004] Piponi, D. (2004). Automatic differentiation, C++ templates, and photogrammetry. *Journal of Graphics Tools*, 9(4):41–55.

[Price, 1991] Price, G. B. (1991). *An introduction to multicomplex spaces and functions*, volume 140. CRC Press.

[Reddy and Trefethen, 1994] Reddy, S. C. and Trefethen, L. N. (1994). Pseudospectra of the convection-diffusion operator. *SIAM Journal on Applied Mathematics*, 54(6):1634–1649.

[Rincon-Camacho et al., 2014a] Rincon-Camacho, M. M., Chatelin, F., and Ricoux, P. (2014a). About a family of logistic equation based on a relative distance to $\frac{1}{2}$ raised to a positive power. Technical report, CERFACS TR/PA/14/55.

[Rincon-Camacho et al., 2014b] Rincon-Camacho, M. M., Chatelin, F., and Ricoux, P. (2014b). About relative and absolute logic evolutions under laws of degree 2 and 4 and in 4 dimensions at most. Technical report, CERFACS TR/PA/14/75.

[Rincon-Camacho et al., 2014c] Rincon-Camacho, M. M., Chatelin, F., and Ricoux, P. (2014c). Beyond Boolean logic. A family of logistic equations as a model for numerical evolution of the fixed points 0 and 1 for multiplication. Technical report, CERFACS TR/PA/14/68.

[Rincon-Camacho and Latre, 2013] Rincon-Camacho, M. M. and Latre, J.-B. (2013). Project description: Algebraic structures for information processing associated with Dickson algebras. Technical report, CERFACS TR/PA/13/106.

[Scheffers, 1893] Scheffers, M. (1893). Sur la généralisation des fonctions analytiques. *CR Acad. Sc*, 116:1114.

[Sobczyk, 1995] Sobczyk, G. (1995). The hyperbolic number plane. *The College Mathematics Journal*, 26(4):268–280.

[Study, 1903] Study, E. (1903). Geometrie der Dynamen.

[Torsello et al., 2011] Torsello, A., Rodola, E., and Albarelli, A. (2011). Multiview registration via graph diffusion of dual quaternions. In *Computer Vision and Pattern Recognition (CVPR), 2011 IEEE Conference on*, pages 2441–2448. IEEE.

[Vaillant et al., 2013] Vaillant, R., Barthe, L., Guennebaud, G., Cani, M.-P., Rohmer, D., Wyvill, B., Gourmel, O., and Paulin, M. (2013). Implicit skinning: Real-time skin deformation with contact modeling. *ACM Transaction on Graphics (TOG). Proceedings of ACM SIGGRAPH.*

[van Vlaenderen and Waser, 2001] van Vlaenderen, K. J. and Waser, A. (2001). Generalisation of classical electrodynamics to admit a scalar field and longitudinal waves. *Hadronic Journal*, 24(5):609–628.

[Veldkamp, 1976] Veldkamp, G. (1976). On the use of dual numbers, vectors and matrices in instantaneous, spatial kinematics. *Mechanism and Machine Theory*, 11(2):141–156.

[Wu et al., 2005] Wu, Y., Hu, X., Hu, D., Li, T., and Lian, J. (2005). Strapdown inertial navigation system algorithms based on dual quaternions. *Aerospace and Electronic Systems, IEEE Transactions on*, 41(1):110–132.

[Wu et al., 2006] Wu, Y., Hu, X., Wu, M., and Hu, D. (2006). Strapdown inertial navigation using dual quaternion algebra: error analysis. *Aerospace and Electronic Systems, IEEE Transactions on*, 42(1):259–266.

[Yaglom, 1968] Yaglom, I. (1968). Complex numbers in geometry. Translated from the Russian by Eric J. F. Primrose. Academic Press, New York.

[Yang and Freudenstein, 1964] Yang, A. T. and Freudenstein, F. (1964). Application of dual-number quaternion algebra to the analysis of spatial mechanisms. *Journal of Applied Mechanics*, 31(2):300–308.